

Heat Transfer & Periodic Flow Analysis of Heat Exchanger by CFD with Nano Fluids

Ms. N.Gayathri¹, Mr.V.V.Ramakrishna M.Tech², Mr. Sanmala Rajasekhar³
M.Tech(P.Hd)

¹ M.Tech Student Department Of Mechanical Engg, KITS Engineering College, Divilia.P, India, 533433.

² Asst Professor Department Of Mechanical Engg, KITS Engineering College, Divili, A.P, India, 533433.

³ Assoc.Professor Department Of Mechanical Engg, KITS Engineering College, Divilia.P, India, 533433.

Abstract

Many heat transfer applications such as steam generators in a boiler or air cooling coil of an air conditioner, can be modelled in a bank of tubes containing a fluid flowing at one temperature that is immersed in a second fluid in a cross flow at different temperature. CFD simulations are a useful tool for understanding flow and heat transfer principles as well as for modelling these types of geometries. Both the fluids considered in the present study are CUO Nano fluids, and flow is classified as laminar and steady with Reynolds number between 100-600. The mass flow rate of the cross flow and diameter has been varied (such as 0.05, 0.1, 0.15, 0.20, 0.25, 0.30 kg/sec and 0.8, 1.0, 1.2 & 1.4cm) and the models are used to predict the flow and temperature fields that result from convective heat transfer. Due to symmetry of the tube bank and the periodicity of the flow inherent in the tube bank geometry, only a portion of the geometry will be modelled and with symmetry applied to the outer boundaries. The inflow boundary will be redefined as a periodic zone and the outflow boundary is defined as the shadow. The various static pressures, velocities, and temperatures obtained are reported.

In this present project tubes of different diameters and different mass flow rates are considered to examine the optimal flow distribution. Further the problem has been subjected to effect of materials used for tubes manufacturing on heat transfer rate. Materials considered are copper and Nickle Chromium alloys. Results emphasize the utilization of alloys in place of copper as tube material serves better heat transfer with most economical way.

Keywords: Heat transfer, Heat exchanger, Nano fluids, Mass flow rate, Periodic flow, Nusselt number & Reynolds number.

I. Introduction

Generally in any kind of heat exchanger the commonly used flowing fluid is water. But now here we are using Nano fluid (CUO). A Nano fluid is a fluid containing nanometre-sized particles, called nanoparticles. These fluids are engineered colloidal suspensions of nanoparticles in a base fluid. The nanoparticles used in Nano fluids are typically made of metals, oxides, carbides, or carbon nanotubes. Common base fluids include water, ethylene glycol and oil.

Nano fluids have novel properties that make them potentially useful in many applications in heat transfer including microelectronics, fuel cells, pharmaceutical processes, and hybrid –powered engines, engine cooling/vehicle thermal management, domestic refrigerator, chiller, heat exchangers in grinding, machining and in boiler flue gas temperature reduction. They exhibit enhanced thermal conductivity and the convective heat transfer coefficient compared to the base fluid. Knowledge of the rheological behaviour of Nano fluids is found to be very critical in deciding their suitability for convective heat transfer

applications. In analysis such as computational fluid dynamics (CFD), Nano fluids can be assumed to be single phase fluids. However, almost all of new academic paper uses two-phase assumption. Classical theory of single phase fluids can be applied, where physical properties of Nano fluids are taken as a function of properties of both constituents and their concentrations. An alternative approach simulates Nano fluids using a two-component model. The spreading of a Nano fluid droplet is enhanced by the solid-like ordering structure of nanoparticles assembled near the contact line by diffusion, which gives rise to a structural disjoining pressure in the vicinity of the contact line. However, such enhancement is not observed for small droplets with diameter of nanometre scale, because the wetting time scale is much smaller than the diffusion time scale.

1.1 Synthesis

Nano fluids are produced by several techniques they are,

1. Direct Evaporation (1 step),
2. Gas condensation/dispersion (2 step),

3. Chemical vapour condensation (1 step),
4. Chemical precipitation (1 step).

Several liquids including water, ethylene glycol, and oils have been used as base fluids. Nano-materials used so far in Nano fluid synthesis include metallic particles, oxide particles, carbon nanotubes, graphene Nano-flakes and ceramic particles

1.2 Applications

Nano fluids are primarily used as coolant in heat transfer equipment such as heat exchangers, electronic cooling system (such as flat plate) and radiators. Heat transfer over flat plate has been analysed by many researchers. Graphene based Nano fluid has been found to enhance polymerase chain reaction efficiency. Nano fluids in solar collectors are another application where Nano fluids are employed for their tenable optical properties.

II. Simulation & Need for CFD

2.1 Simulation

'Simulation' is the imitation of the operation of a real-world process or system over time. The act of simulating something first requires that a model to be developed. This model represents the key characteristics or behaviours of the selected physical system or abstract system or process. The model represents the system itself, whereas the simulation represents the operation of the system over time.

Simulation is an important feature in engineering system or any other system that involves many processes. For example in electrical engineering, delay lines may be used to simulate propagation delay and phase shift caused by an actual transmission line. Similarly, dummy loads may be used to simulate impedance without simulating propagation, and is used in situations where propagation is unwanted. A simulator may imitate only a few of the operations and functions of the unit it simulates. *Contrast with:* emulate.

Most engineering simulations entail mathematical modelling and computer assisted investigation. There are many cases, however, where mathematical modelling is not reliable. Simulations of fluid dynamics problems often require both mathematical and physical simulations. In these cases the physical models require dynamic similitude. Physical and chemical simulations have also direct realistic uses, rather than research uses. For example in chemical engineering, process simulations are used to give the process parameters immediately used for operating chemical plants such as oil refineries.

Simulations can be categorised in different ways. Some of them are as follows:

1. *Physical simulation* refers to simulation in which physical objects are substituted for the real thing.

These physical objects are often chosen because they are smaller or cheaper than the actual object or system.

2. *Interactive simulation* is a special kind of physical simulation, often referred to as a *human in the loop* simulation, in which physical simulations include human operators, such as in a flight simulator or a driving simulator. Human in the loop simulations can include a computer simulation as a so-called *synthetic environment*.

There are more different types of simulations according to the field or stream suiting for research. Here we are using engineering simulation with the help of Computational Fluid Dynamics (CFD) software.

2.2 Need for CFD

Conventional engineering analyses rely heavily on empirical correlations so it is not possible to obtain the results for specific flow and heat transfer patterns in heat exchanger of arbitrary geometry. Successful modeling of such process lies on quantifying the heat, mass and momentum transport phenomena. Today's design processes must be more accurate while minimizing development costs to compete in a world of economy. This forces engineering companies to take advantage of design tools which augment existing experience and empirical data while minimizing cost. One tool which excels under these conditions is CFD.

Computational Fluid Dynamics (CFD) makes it possible to solve numerically the flow and energy balances in complicated geometries. CFD simulates the physical flow, heat transfer, and combustion phenomena of solids, liquids, and gases and executing on high speed, large memory workstations. CFD has significant cost advantages when compared to physical modeling and field testing and also, provides additional insight into the physical phenomena being analyzed due to the availability of data that can be analyzed and the flexibility with which geometric changes can be studied. Effective heat transfer parameters estimated from CFD results matched theoretical model predictions reasonably well. Heat exchangers have been extensively researched both experimentally and numerically. However, most of the CFD simulation on heat exchangers was aimed at model validation.

2.3 Simulation phenomena in heat exchangers

Hilde VAN DER VYVER, Jaco DIRKER AND Jousa P. MEYER, who investigated the validation of a CFD model of a three dimensional Tube-in-Tube Heat Exchanger. The heat transfer coefficients and the friction factors were determined with CFD and compared to established correlations. The results showed the reasonable agreement with empirical correlation, while the trends were similar. When

compared with experimental data the CFD model results showed good agreement. The average error was 5.5% and the results compared well with

correlation. It can be concluded that the CFD software modelled a Tube-in-Tube Heat Exchanger in three-dimensional accurately.

2.3.1 Shell & Tube Heat Exchanger

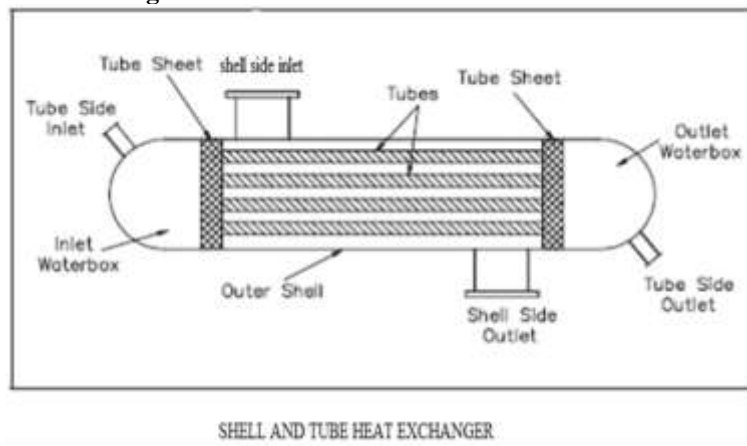


Fig.2.3.1 Heat transfer for heat exchanger.

The second law of thermodynamics states that heat always flows spontaneously from hotter region to a cooler region. All active and passive devices are sources of heat. These devices are always hotter than the average temperature of their immediate surroundings. There are three mechanisms for heat transfer viz, conduction, convection and radiation.

2.3.2 Heat Exchanger Tubes

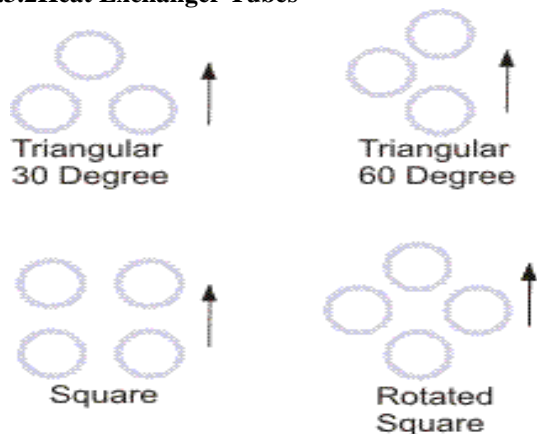


Fig. 2.3.2 common tube layouts for exchangers.

The tubes are the basic components of the shell and Tube heat exchanger, providing the heat transfer surface between on fluid flowing inside the tube and the other fluid flowing across outside of the tubes. The tubes may be seamless or welded and most commonly made of copper or steel alloys. Other alloys for specific applications the tubes are available in a variety of metals which includes admiralty, Mountz metal, brass, 70-30 copper nickel, aluminium bronze, aluminium. They are available in a number of different wall thicknesses. Tubes in heat exchangers

are laid out on either square or triangular patterns as shown in fig.2.3.2. The advantage of square pitch is that the tubes are accessible for external cleaning and cause a lower pressure drop when fluid flows in the direction indicated in the fig.2.3.2.

2.3.3 Shell-side film coefficients

The heat transfer coefficients outside tube bundle are referred to as shell-side coefficients. When the tube bundle employs baffles, which serves two functions: most importantly they support the tubes in the proper position during assembly and operation and prevent vibration of the tubes caused by flow-induced eddies. Secondly they guide the shell-side flow back and forth across the tube field, increasing the velocity and the heat transfer coefficient.

In square pitch, as shown in fig.2.3.2 the velocity of the fluid undergoes continuous fluctuation because of the constricted area between adjacent tubes compared with the flow area between successive rows. In triangular pitch even greater turbulence is encountered because the fluid flowing between adjacent tubes at high velocity impinges directly on the succeeding rows. This indicates that, when the pressure drop and cleavability are of little consequence, triangular pitch is superior for the attainment of high shell-side film coefficients. This is the actually the case, and under comparable conditions of flow and tube size the coefficients for triangular pitch are roughly 25% greater than for square pitch.

2.3.4 Shell-side mass velocity

Shell is simply the container for the shell-side fluid. The shell is commonly has a circular cross section and is commonly made by rolling a metal plate of appropriate dimensions into a cylinder and

welding the longitudinal joint. In large exchangers the shell is made out of carbon steel wherever possible for reasons of economy. Though other alloys can be and are used when corrosion (or) high temperature strength demand must be met. The linear and mass velocities of the fluid change continuously across the bundle, since the width of the shell and number of tube vary from row to row.

2.3.5 Shell-side Pressure Drop

The total pressure, Δp , across a system consists of three components:

- A static pressure difference, ΔP_s , due to the density and elevation of the fluid.

- A pressure differential, ΔP , due to the change of momentum.
- A pressure differential due to frictional losses, ΔP_f .

$$\Delta P_t = \Delta P_s + \Delta P_m + \Delta P_f$$

2.4 Applications of Simulation

- Pulverized Application
- Micronized Coal Nozzle Application
- Coal Gasification Application
- Convection Pass Erosion Application
- Scrubber Applications
- Steam Drum Application etc,

III. Computational Fluid Dynamics

3.1 Designs of optimization problem

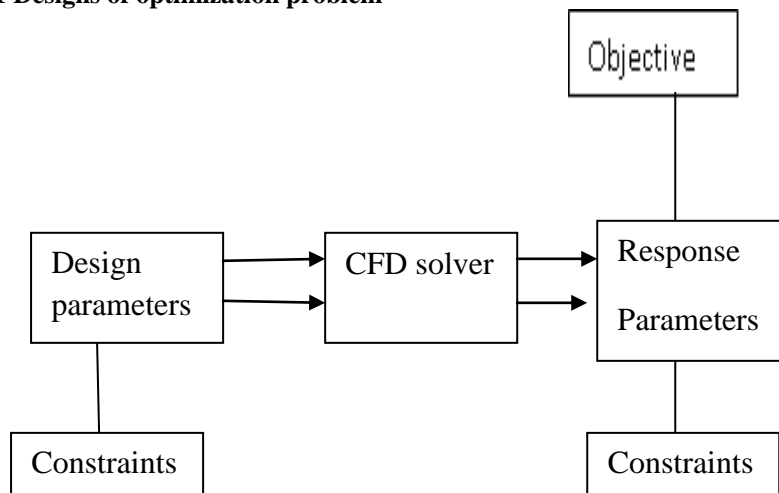


Fig. 3.1 Design of optimization problem

3.2 The strategy of CFD

Broadly, the strategy of CFD is to replace the continuous problem domain with a discrete domain using a grid. In the continuous domain, each flow variable is defined at every point in the domain. For instance, the pressure p in the continuous 1D domain shown in the figure below would be given as $P = p(x); 0 < x < 1$ (3.1)

In the discrete domain, each flow variable is defined only at the grid points. So, in the discrete domain shown below, the pressure would be defined only at the N grid points.

$$P_i = p(x_i); \quad i=1,2,\dots,N \quad (3.2)$$

Continuous	Domain
Discrete Domain	
$0 \leq x \leq 1$	x
$= x_1 + x_2, \dots, x_n$	
$X=0 \quad x=1$	x_1, x_n

Coupled PDEs+ boundary condition Coupled algebraic eqs. in continuous variables in discrete variables

In a CFD solution, one would directly solve for the relevant flow variables only at the grid points. The values at other locations are determined by interpolating the values at the grid points.

The governing partial differential equations and boundary conditions are defined in terms of the continuous variables p, V_i etc. One can approximate these in the discrete domain in terms of the discrete variables p_i, V_i etc. The discrete system is a large set of coupled, algebraic equations in the discrete variables, setting up the discrete system and solving it (which is a matrix inversion problem) involves a very large number of repetitive calculations and is done by the digital computer.

3.3 Physical and Mathematical basis of the CFD

All mathematical simulations are carried out within commercial software package environment, FLUENT. The governing equations solved for the flow fields are the standard conservation equations of mass and momentum in the mathematical simulations. The equation for RTD is a normal

species transportation equation. For trajectories of the inclusion, discrete phase model (DPM) is employed with revised wall boundary conditions. The free surface and tannish walls have different boundary conditions (such as reflection and entrapment) for droplets/solid inclusion particles. Taking the range of inclusion particles' diameter (Chevrier and Cramb, 2005) and the shapes for different types of inclusions (Beskow, et al., 2002) into consideration, the boundaries and drag law for particles are then revised by user defined function (UDF) and shape correction coefficient. During trajectory simulations, Stokes-Cunningham drag law is employed with Cunningham correction. Inclusions sometimes could be liquid phase. It is difficult to set the correction coefficient (Haider and Leve spiel, 1989) exactly since droplets can move and deform continuously. While Sinha and Sahai (1993) set both top free face and walls as trap boundary, Lopez-Ramirez et al. (2001) did not illustrate the boundary conditions for inclusion. Zhang, et al. (2000) divided the tannish into two kinds of separate zones. The walls are set as reflection boundary in this work for comparison of separation ratios of inclusion in SFT and a tundish with TI. Although most of the reports indicate that the free surface is a trap boundary, there is a possibility of re-entrainment (Bouris and Bergeles, 1998) to be considered.

3.4 Fluid Flow Fundamentals

The physical aspects of any fluid flow are governed by three fundamental principles. Mass is conserved; Newton's second law and Energy is conserved. These fundamental principles can be expressed in terms of mathematical equations, which in their most general form are usually partial differential equations. Computational Fluid Dynamics (CFD) is the science of determining a numerical solution to the governing equations of fluid flow whilst advancing the solution through space or time to obtain a numerical description of the complete flow field of interest.

The governing equations for Newtonian fluid dynamics, the unsteady Navier-stokes equations, have been known for over a century. However, the analytical investigation of reduced forms of these equations is still an active area of research as is the problem of turbulent closure for the Reynolds averaged form of the equations. For non-Newtonian fluid dynamics, chemical reacting flows and multiphase flows theoretical developments are at a less advanced stage.

Experimental fluid dynamics has played an important role in validating and delineating the limits of the various approximations to the governing equations. The wind tunnel, for example, as a piece of experimental equipment, provides an effective means of simulating real flows. Traditionally this has

provided a cost effective alternative to full scale measurement. However, in the design of the equipment that depends critically on the flow scale measurement as part of the design process is economically impractical. This situation has led to an increasing interest in the development of a numerical wind tunnel.

3.5 The Governing equations

In the case of steady- two dimensional flow, the continuity (conservation of mass) equation is:

$$\frac{\partial(\rho u)}{\partial x} + \frac{\partial(\rho v)}{\partial y} = 0 \quad (1)$$

For incompressible flow, the momentum equations are the x direction:

$$\rho u \frac{\partial u}{\partial x} + \rho v \frac{\partial u}{\partial y} = -\frac{\partial \rho}{\partial x} + \frac{\partial(2\mu \frac{\partial u}{\partial x})}{\partial x} + \frac{\partial(\mu [\frac{\partial u}{\partial y} + \frac{\partial v}{\partial x}])}{\partial y} \quad (2.a)$$

And for y direction:

$$\rho u \frac{\partial v}{\partial x} + \rho v \frac{\partial v}{\partial y} = -\frac{\partial \rho}{\partial y} - \rho g + \frac{\partial(\mu [\frac{\partial v}{\partial x} + \frac{\partial u}{\partial y}])}{\partial x} + \frac{\partial(2\mu \frac{\partial v}{\partial y})}{\partial y}, \quad (2.b)$$

The energy conservation equation for the fluid, neglecting viscous dissipation and compression heating, is:

$$\rho C_p (u \frac{\partial T}{\partial x} + v \frac{\partial T}{\partial y}) = \frac{\partial(k \frac{\partial T}{\partial x})}{\partial x} + \frac{\partial(k \frac{\partial T}{\partial y})}{\partial y} \quad (3)$$

The above equations are called **Naiver-Stokes**. And these are solved using a standard well-verified discretization technique which in turn forms algebraic equations. These equations particularly suited for CFD. The following section illustrates the discretization techniques.

3.6 Method of solution

- Discretization
- Explicit and Implicit Schemes
- Stability Analysis

Some points to note:

1. CFD codes will allow you to set the Courant number (which is also referred to as the CFL number) when using time-stepping. Taking larger time-steps leads to faster convergence to the steady state, so it is advantageous to set the Courant number as large as possible within the limits of stability.
2. A lower courant number is required during start-up when changes in the solution are highly nonlinear but it can be increased as the solution progresses.
3. Under- relaxation for non-time stepping.

3.7 Fluent as a modelling and analysis tool

In parallel with the construction of physical models, a succession of computational fluid dynamics (CFD) models were developed during the prototype design phase. The software chosen for numerical modelling in this project was fluent. The software was easily learned and very flexible in use. Boundary conditions could be set up quickly and the

software could rapidly solve problems involving complex flows ranging from incompressible (low subsonic) to mildly compressible (Transonic) to highly compressible (Supersonic) flows. The wealth of physical models in Fluent allows to accurately predicting laminar and turbulent flows, various modes of heat transfer. Chemical reactions, multiphase flows, and other phenomena with complete mesh flexibility and solution based mesh adoption.

The governing partial differential equations for the conservation of momentum and scalars such as mass, energy and turbulence are solved in the integral form. Fluent uses a control-volume based technique. The governing equations are solved sequentially. The fact that these equations are coupled makes it necessary to perform several iterations of the solution loop before convergence can be reached. The solution loop consists of seven steps that are performed in order.

- The momentum equations for all directions are each solved using the current pressure values (initially the boundary condition is used), in order to update the velocity field.
- The obtained velocities may not satisfy the continuity equation locally. Using the continuity equation and the linear zed momentum equation a 'Poisson-type' equation for pressure correction is derived. Using this pressure correction the pressure and velocities are corrected to achieve continuity.
- K and ϵ equations are solved with corrected velocity field.
- All other equations (energy, species conservation etc.) are solved using the corrected values of the variables.
- Fluid properties are updated.
- Any additional inter-phase source terms are updated.
- A check for convergences is performed.

These seven steps are continued until in the last step the convergence criteria are met.

3.8 Imposing Boundary Conditions

The boundary conditions determine the flow and thermal variables on the boundaries of the physical model. There are a number of classifications of boundary conditions:

- Flow inlet and exit boundaries: pressure inlet, velocity inlet, inlet vent, intake fan, pressure outlet, out flow, outlet fan, and exhaust fan.
- Wall, repeating, and pole boundaries: wall, symmetry, periodic, and axis.
- Internal cell zone: fluid, solid.
- Internal face boundaries: fan, radiator, porous jump, wall, interior.

With the determination of the boundary conditions the physical model has been defined and numerical solution will be provided.

IV. Modelling of periodic flow using gambit and fluent

4.1 Introduction

Many industrial applications, such as steam generation in a boiler, air cooling in the coil of air conditioner and different type of heat exchangers uses tube banks to accomplish a desired total heat transfer.

The system considered for the present problem, consisted bank of tubes containing a flowing fluid at one temperature that is immersed in a second fluid in cross flow at a different temperature. Both fluids are water, and the flow is classified as laminar and steady, with a Reynolds number of approximately 100. The mass flow rate of cross flow is known, and the model is used to predict the flow and temperature fields that result from convective heat transfer due to the fluid flowing over tubes.

The figure depicts the frequently used tube banks in staggered arrangements. The situation is characterized by repetition of an identical module shown as transverse tubes. Due to symmetry of the tube bank, and the periodicity of the flow inherent in the tube geometry, only a portion of the geometry will be modelled as two dimensional periods' heat flows with symmetry applied to the outer boundaries.

4.2 CFD modelling of a periodic model

- Creating physical domain and meshing
- Creating periodic zones
- Set the material properties and imposing boundary conditions
- Calculating the solutions using segregated solver.

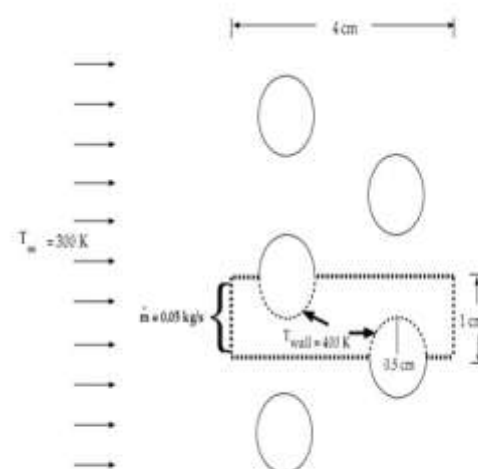


Fig. 4.3.1.Schematic diagram of the problem

The modelling and meshing package used is GAMBIT. The geometry consists of a periodic inlet and outlet boundaries, tube walls. The bank consists of uniformly spaced tubes with a diameter D, which are staggered in the direction of cross flow. Their centres are separated by a distance of 2cm in x-direction and 1 cm in y-direction.

The periodic domain shown by dashed lines in fig 4.3.1.is modelled for different tube diameter viz., D=0.8cm, 1.0cm, 1.2cm and 1.4cm while keeping the

same dimensions in the x and y direction. The entire domain is meshed using a successive ratio scheme with quadrilateral cells. Then the mesh is exported to FLUENT where the periodic zones are created as the inflow boundary is redefined as a periodic zone and the outer flow boundary defined as its shadow, and to set physical data, boundary condition. The resulting mesh for four models is shown in fig 4.3.2

4.3 Modelling details and meshing

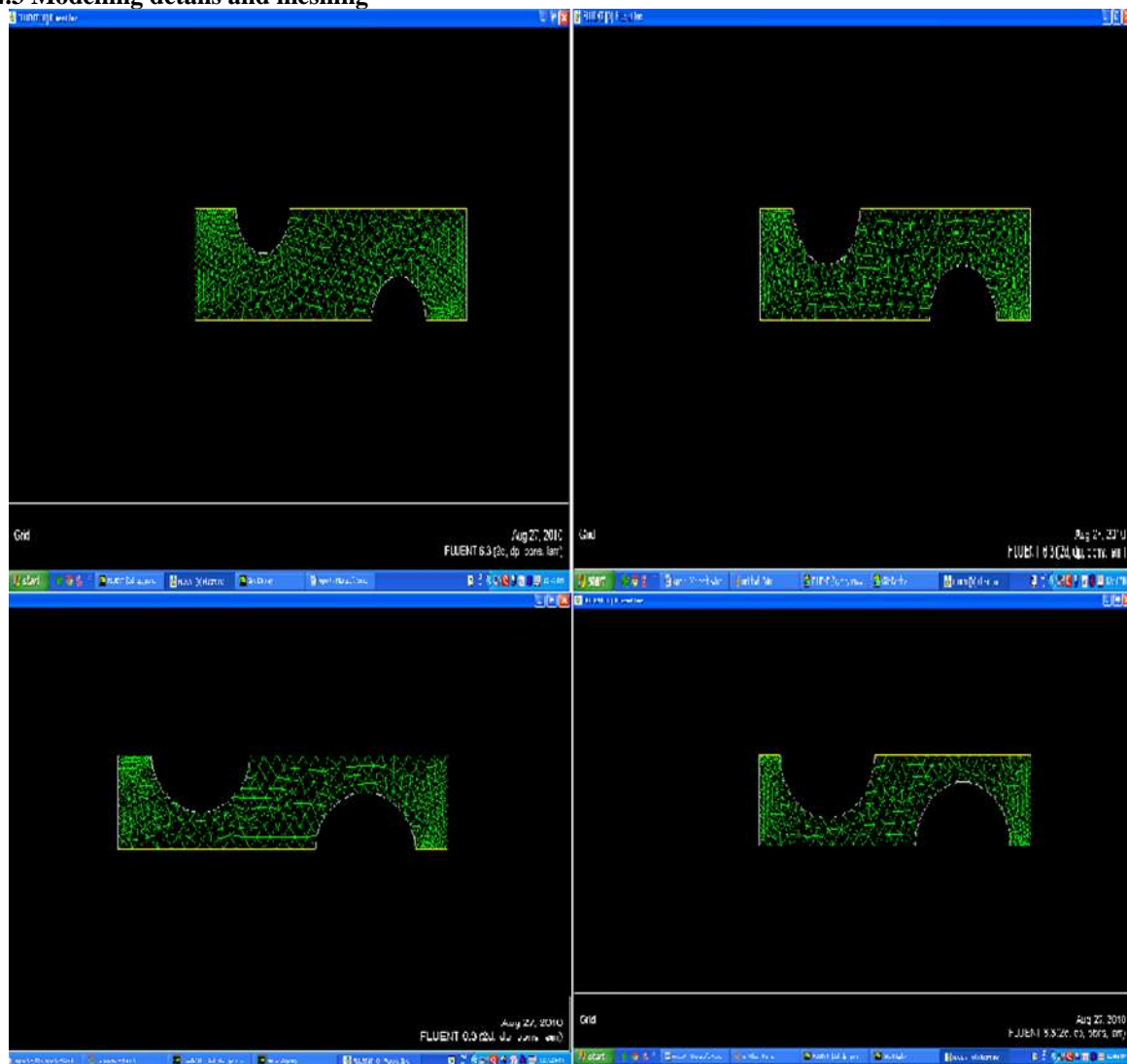


Fig. 4.3.2 Mesh for the periodic tube of diameters 0.8, 1.0, 1.2, 1.4cm

4.4 Material properties and boundary conditions

The material properties of working fluid (water) flowing over tube bank at bulk temperature of 300K, are:

$$\rho = 998.2\text{kg/m}^3$$

$$\mu = 0.001003\text{kg/m-s}$$

$$C_p = 4182 \text{ J/kg-k}$$

$$K = 0.6 \text{ W/m-k}$$

4.4.1 Boundary conditions assigned in FLUENT

The boundary conditions applied on physical domain are as follows

Fluid flow is one of the important characteristic of a tube bank. It is strongly effects the heat transfer process of a periodic domain and its overall performance. In this paper, different mass flow rates at free stream temperature, 300K were used and the wall temperature of the tube which was treated as heated section was set at 400K as periodic boundary conditions for each model which are tabulated as follows

4.4.2 Mass flow rates for different tube diameter

Tube diameter(D) (cm)	Periodic condition (Kg/s)
0.8	m=0.05-0.30
1.0	m=0.05,0.30
1.2	m=0.05-0.30
1.4	m=0.05-0.30

The wall temperature of the tube which was treated as heated section was set at 400k.

4.5 Solution using Segregate Solver

The computational domain was solved using the solver settings as segregated, implicit, two-dimensional and steady state condition. The numerical simulation of the Naiver Stokes equations, which governs the fluid flow and heat transfer, make use of the finite control volume method. CFD solved for temperature, pressure and flow velocity at every cell. Heat transfer was modelled through the energy equation. The simulation process was performed until the convergence and an accurate balance of mass and energy were achieved. The solution process is iterative, with each iteration in a steady state problem. There are two main iteration parameters to be set before commencing with the simulation. The under-relaxation factor determines the solution adjustment for each iteration; the residual cut off value determines when the iteration process can be terminated. The under-relaxation factor is an arbitrary number that determines the solution adjustment between two iterations, a high factor will result in a large adjustment and will result in a fast convergence, if the system is stable. In a less stable or particularly nonlinear system, for example in some turbulent flow

or high- Rayleigh-number natural convection cases, a high under-relaxation may lead to divergence, an

Boundary	Assigned as
Inlet	Periodic
Outlet	Periodic
Tube walls	Wall
Outer walls	Symmetry

increase in error. It is

therefore necessary to adjust the under- relaxation factor specifically to the system for which a solution is to be found. Lowering the under-relaxation factor in these unstable systems will lead to a smaller step change between the iterations, leading to less adjustment in each step. This slows down the iterations process but decreases the chance for divergence of the residual values.

The second parameter, the residual value, determines when a solution is converged. The residual value (a difference between the current and former solution value) is taken as a measure for convergence. In a infinite precision process the residuals will go to zero as the process converges. On actual computers the residuals decay to a certain small value (round-off) and then stop changing. This decay may be up to six orders of magnitude for single precision computations. By setting the upper limit of the residual values the ‘cut-off’ value for convergence is set. When the set value is reached the process is considered to have reached its ‘round-off’ value and the iteration process is stopped.

Finally the under-relaxation factors and the residual cut-off values are set. Under- relaxation factors were set slightly below their default values to ensure stable convergence. Residual values were kept at their default values, $1.0e^{-6}$ for the energy residual, $1.0e^{-3}$ for all others, continuity, and velocities. The residual cut-off value for the energy balance is lower because it tends to be less stable than the other balances; the lower residual cut-off ensures that the energy solution has the same accuracy as the other values.

V. Resulting plots/Graphs & Tables

5.1 Convergence plot for different mass flow rates with diameter D=0.8cm

Here we are representing the resultant values for only one diameter i.e; D=0.8cm with different mass flow rate values (i.e; m=0.05, 0.10, 0.15, 0.20, 0.25, & 0.30kg/s) we got the other results for other diameters also but not representing here.

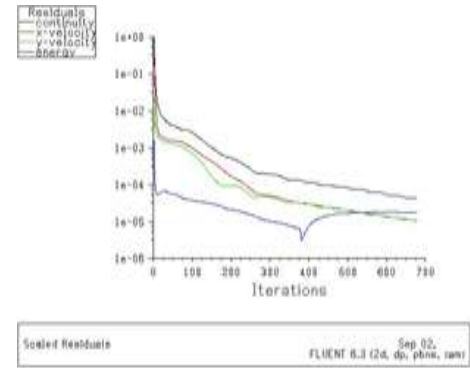
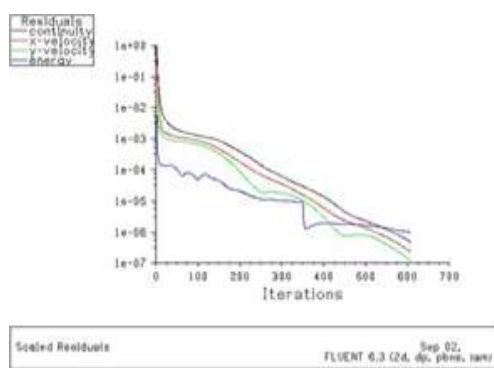


Fig.5.1.1 convergence plot for tube D=0.8cm, m=0.05kg/s Fig.5.1.2 D=0.8cm, m=0.10kg/s

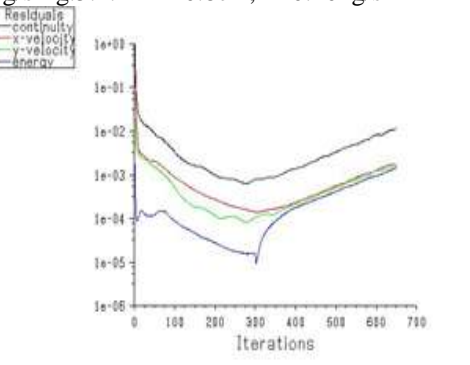
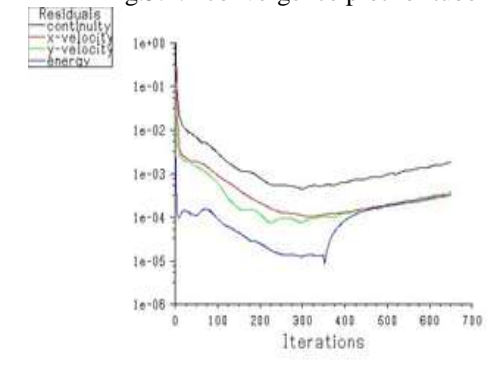


Fig.5.1.3 D=0.8cm, m=0.15kg/s Fig.5.1.4 D=0.8cm, m=0.20kg/s

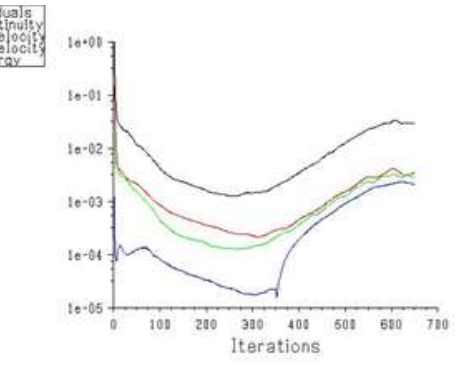
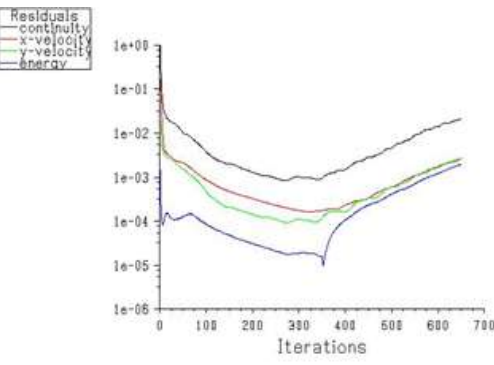


Fig.5.1.5 D=0.8cm, m=0.25kg/s Fig.5.1.6 D=0.8cm, m=0.30kg/s

Similarly we got the results for other diameters with the different mass flowrate values

VI. Results through CFD

6.1 Variation of static pressure for different mass flow rates with diameter D=0.8cm

Here we are representing the resultant values for only one diameter i.e; D=0.8cm with different mass flow rate values (i.e; m=0.05, 0.10, 0.15, 0.20, 0.25, & 0.30kg/s) we got the other results for other diameters also but not representing here.

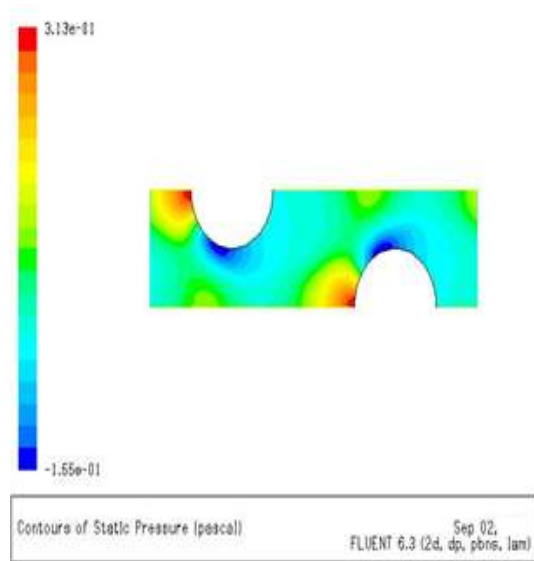
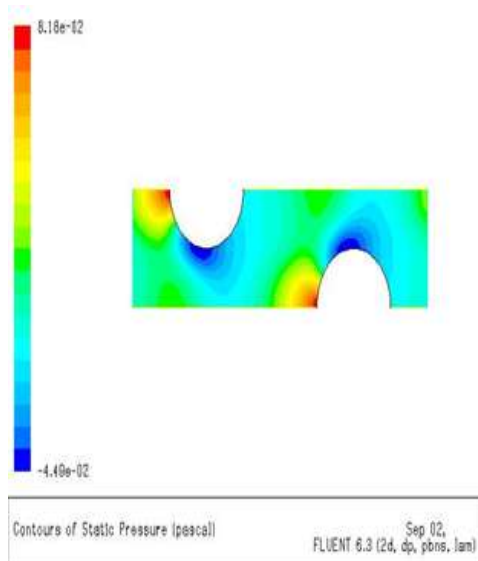


Fig. 6.1.1 D=0.8cm, m=0.05kg/s / Fig.6.1.2 D=0.8cm, m=0.10kg/s

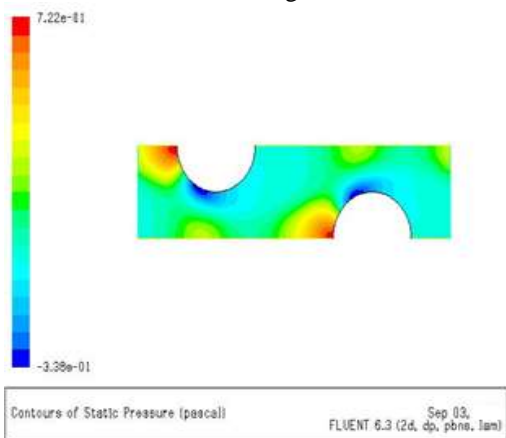


Fig. 6.1.3 D=0.8cm, m=0.15kg/s

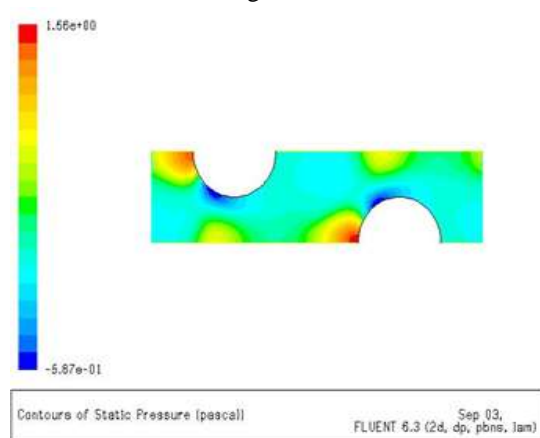


Fig.6.1.4 D=0.8cm, m=0.20kg/s

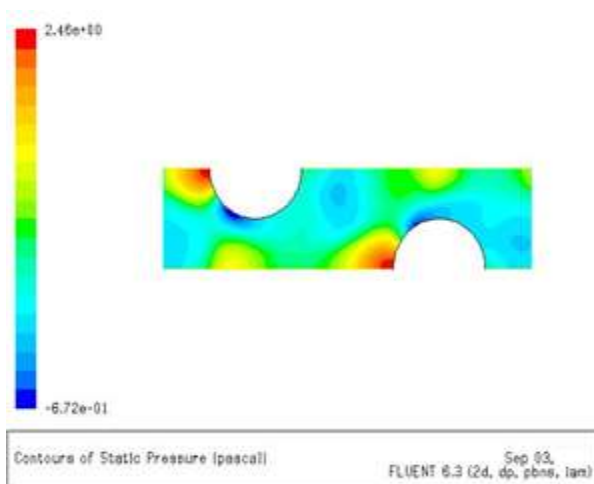


Fig. 6.1.5 D=0.8cm, m=0.25kg/s

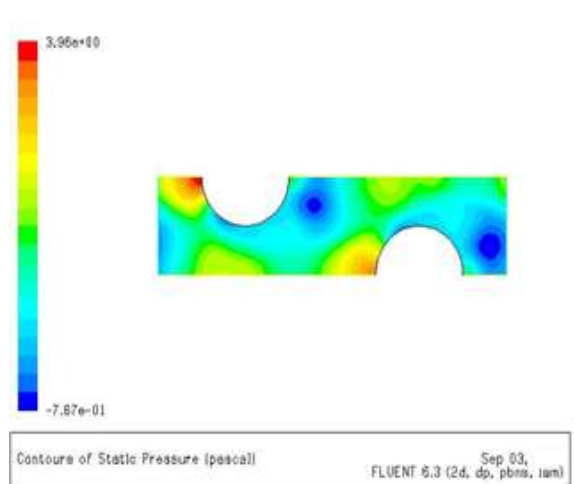


Fig.6.1.6 D=0.8cm, m=0.30kg/s

6.2 Static Temperature for different mass flow rates with diameter D=0.8cm

Here we are representing the resultant values for only one diameter i.e; D=0.8cm with different mass flow rate values (i.e; m=0.05, 0.10, 0.15, 0.20, 0.25, & 0.30kg/s) we got the other results for other diameters also but not representing here.

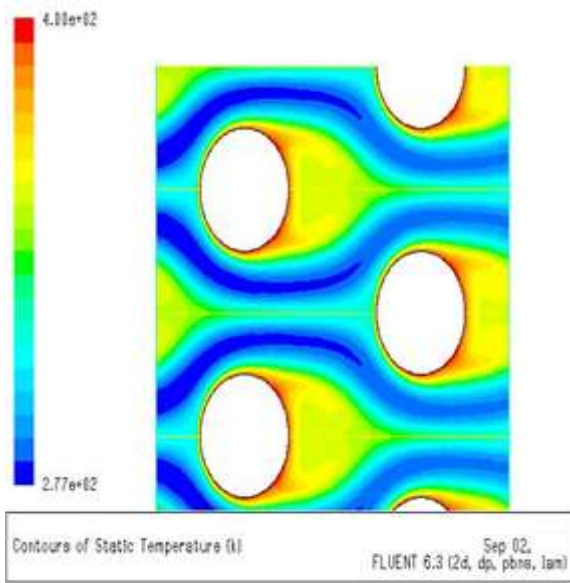


Fig.6.2.1 D=0.8cm,m=0.05kg/s

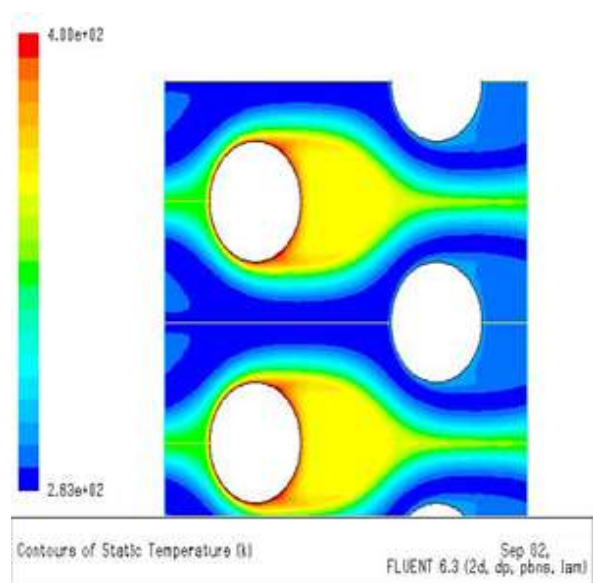


Fig.6.2.2.D=0.8cm,m=0.10kg/s

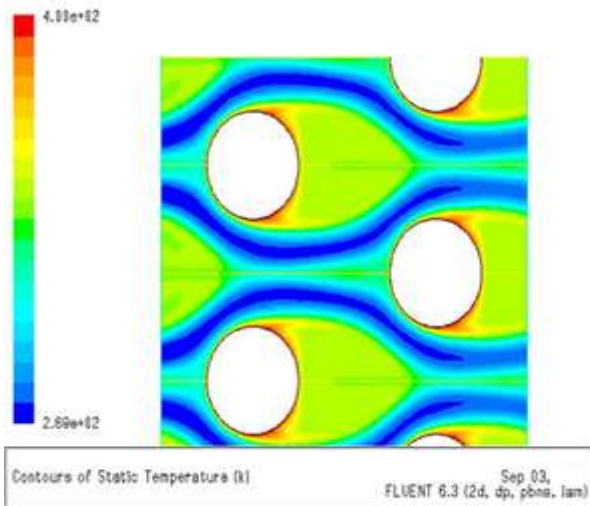


Fig. 6.2.3 D=0.8cm,m=0.15kg/s

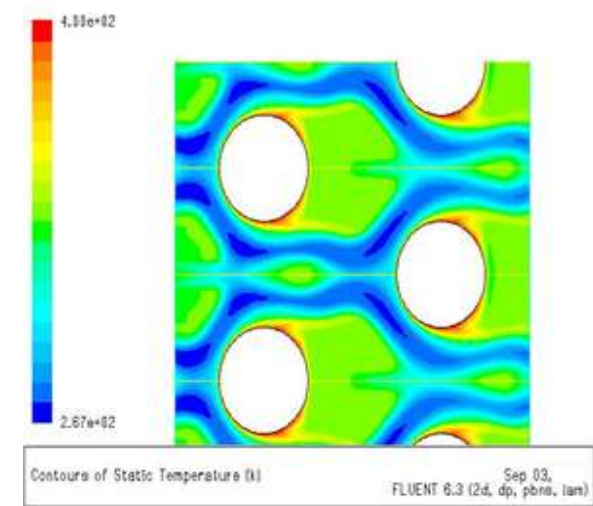


Fig.6.2.4 D=0.8cm,m=0.20kg/s

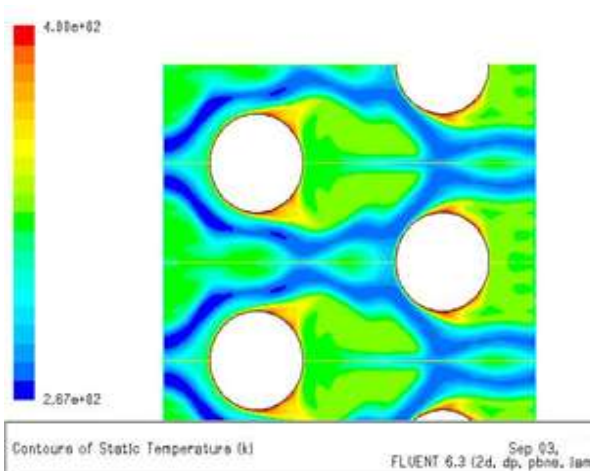


Fig. 6.2.5 D=0.8cm,m=0.25kg/

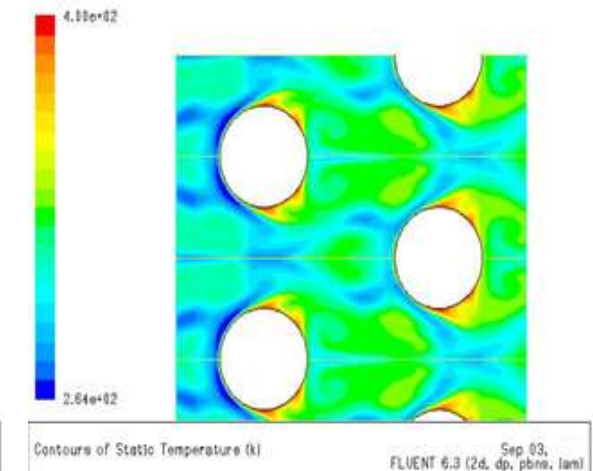


Fig.6.2.6 D=0.8cm,m=0.30kg/s

6.3.1 Velocity vector for different mass flow rates with diameter D=0.8cm

Here we are representing the resultant values for only one diameter i.e; $D=0.8\text{cm}$ with different mass flow rate values (i.e; $m=0.05, 0.10, 0.15, 0.20, 0.25, \& 0.30\text{kg/s}$) we got the other results for other diameters also but not representing here.

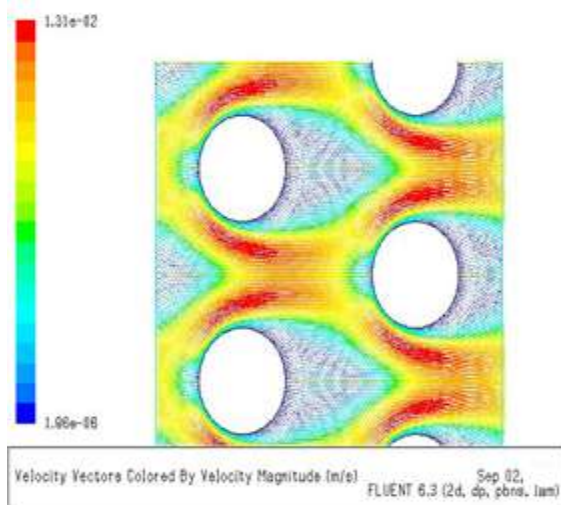


Fig.6.3.1 $D=0.8\text{cm}, m=0.05\text{kg/s}$

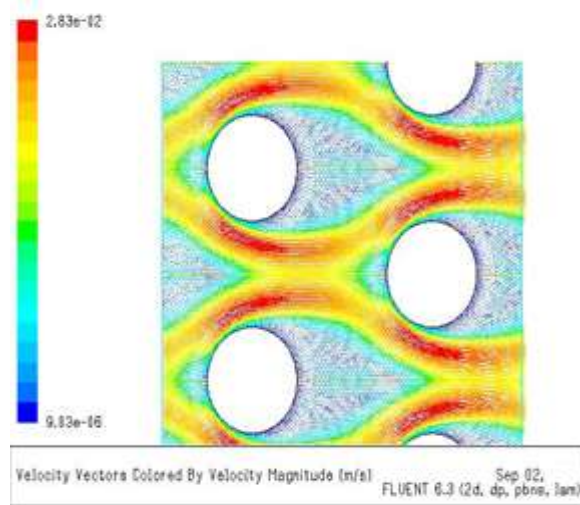


Fig.6.3.2 $D=0.8\text{cm}, m=0.10\text{kg/s}$

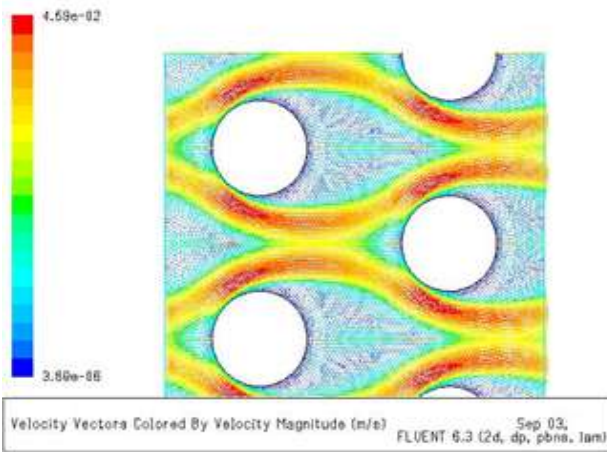


Fig.6.3.3 $D=0.8\text{cm}, m=0.15\text{kg/s}$

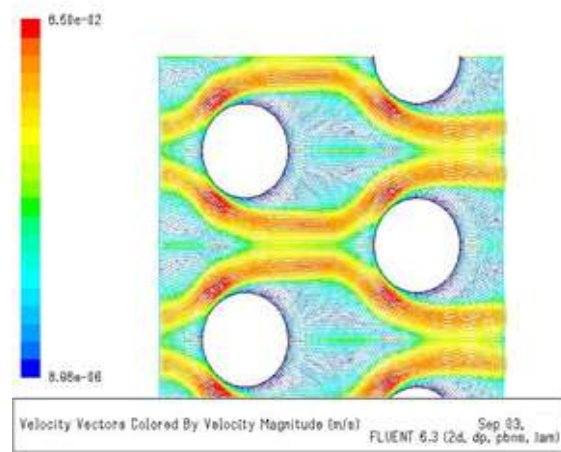


Fig.6.3.4 $D=0.8\text{cm}, m=0.20\text{kg/s}$

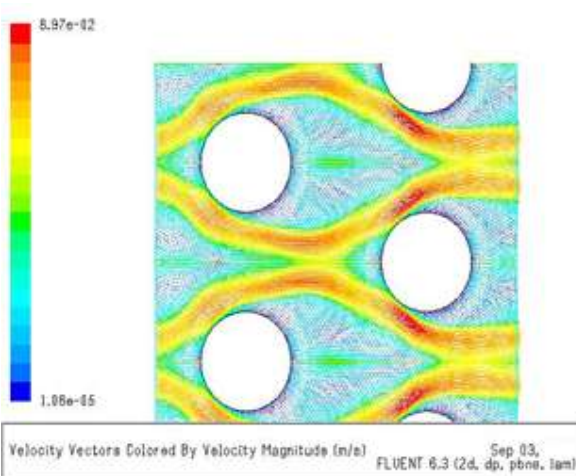


Fig.6.3.5 $D=0.8\text{cm}, m=0.25\text{kg/s}$

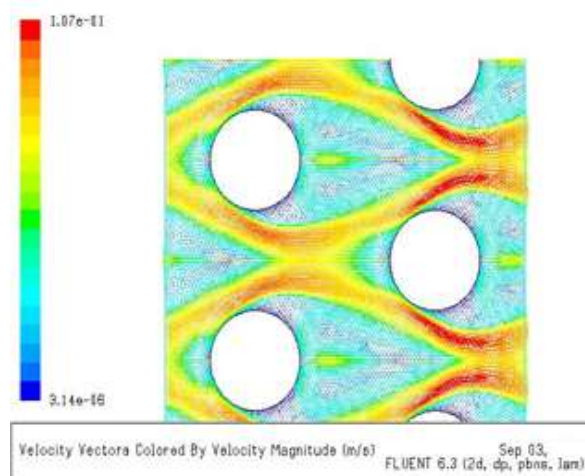


Fig.6.3.6 $D=0.8\text{cm}, m=0.30\text{kg/s}$

6.4 Static Pressure for different mass flow rates with diameter $D=0.8\text{cm}$

Here we are representing the resultant values for only one diameter i.e; $D=0.8\text{cm}$ with different mass flow rate values (i.e; $m=0.05, 0.10, 0.15, 0.20, 0.25, \& 0.30\text{kg/s}$) we got the other results for other diameters also but not representing here.

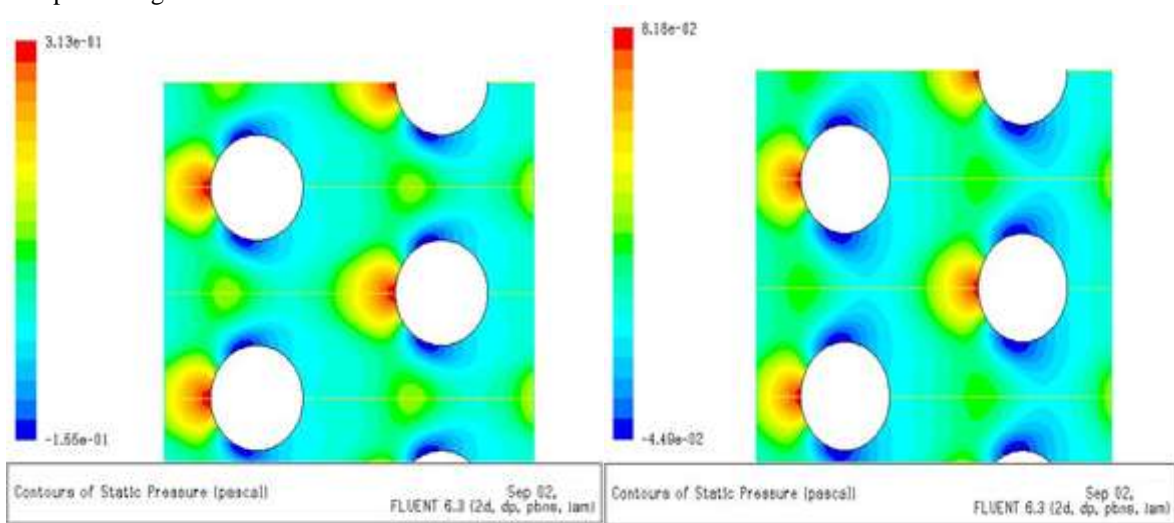


Fig.6.4.1.D=0.8cm,m=0.05kg/s

Fig.6.4.2.D=0.8cm,m=0.10kg/s

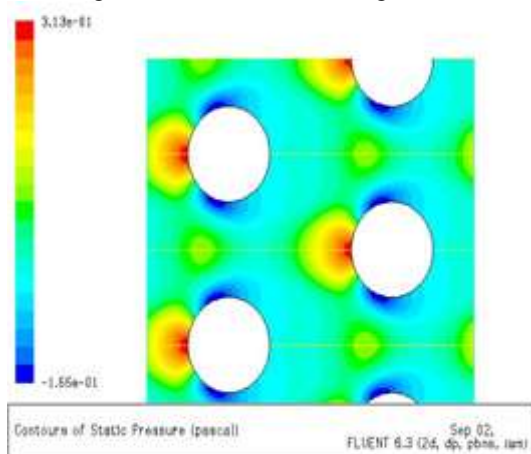


Fig.6.4.3.D=0.8cm,m=0.15kg/s

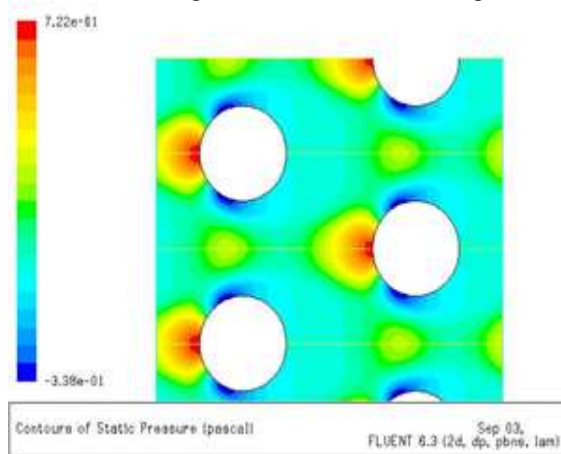


Fig.6.4.4.D=0.8cm,m=0.20kg/s

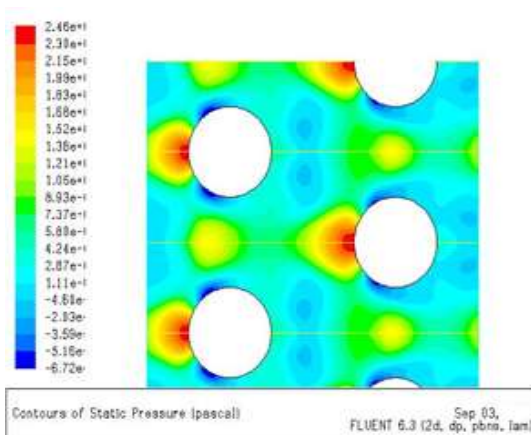


Fig.6.4.5.D=0.8cm,m=0.25kg/s

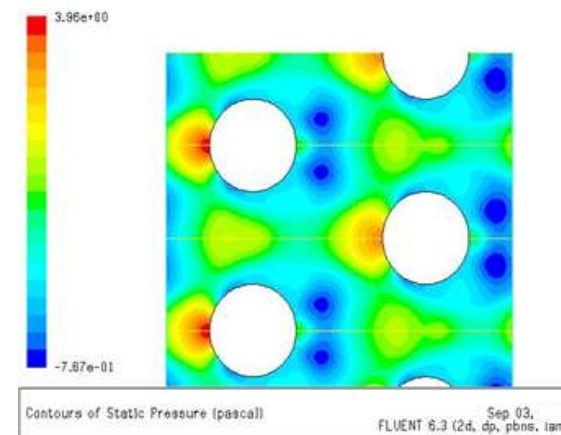
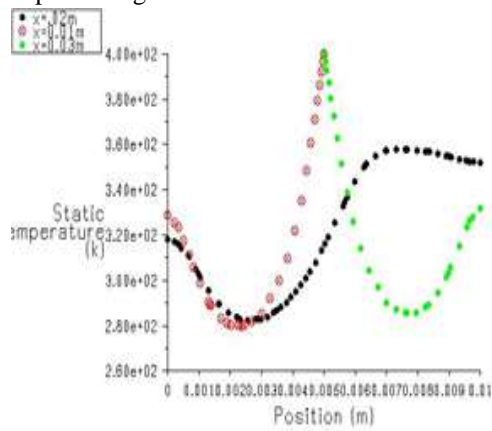


Fig.6.4.6.D=0.8cm,m=0.30kg/s

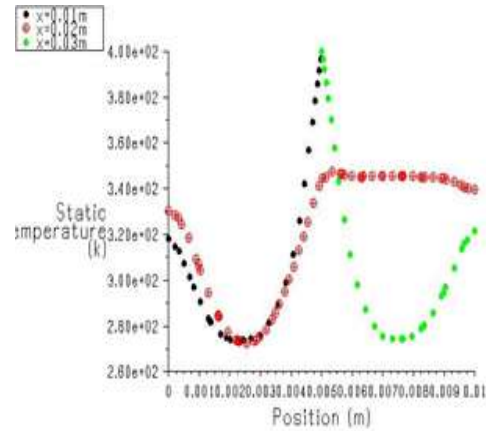
6.5 Static temperature variation in y-axis for different mass flow rates with diameter $D=0.8\text{cm}$

Here we are representing the resultant values for only one diameter i.e; $D=0.8\text{cm}$ with different mass flow rate values (i.e; $m=0.05, 0.10, 0.15, 0.20, 0.25, \& 0.30\text{kg/s}$) we got the other results for other diameters also but not representing here.



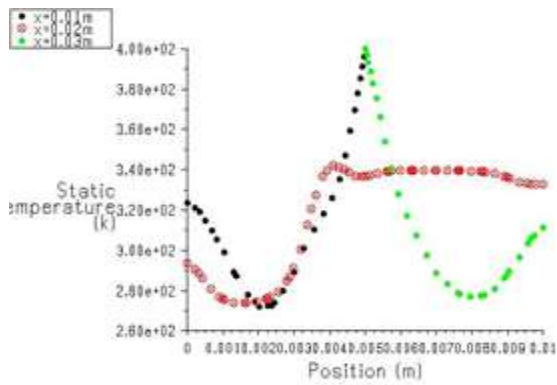
Static Temperature FLUENT 6.3 (2d, dp, pbns, iam) Sep 02,

Fig.6.5.1.D=0.8cm,m=0.05kg/s



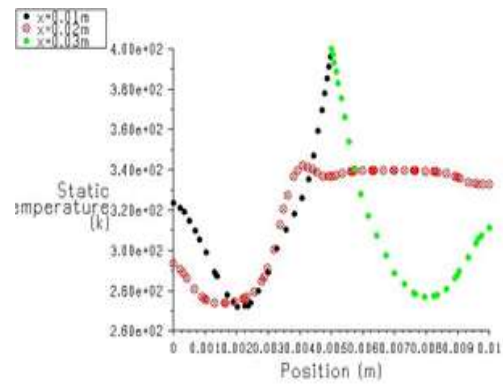
Static Temperature FLUENT 6.3 (2d, dp, pbns, iam) Sep 03,

Fig.6.5.2.D=0.8cm,m=0.10kg/s



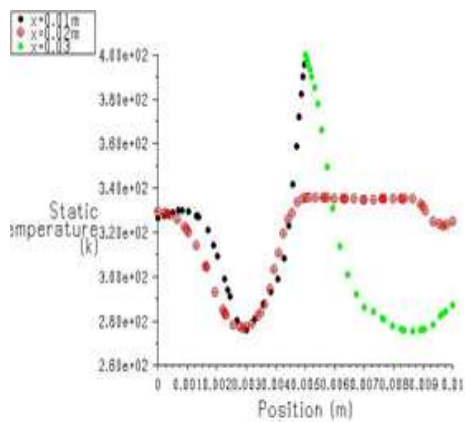
Static Temperature: FLUENT 6.3 (2d, dp, pbns, iam) Sep 03,

Fig.6.5.3.D=0.8cm,m=0.15kg/s



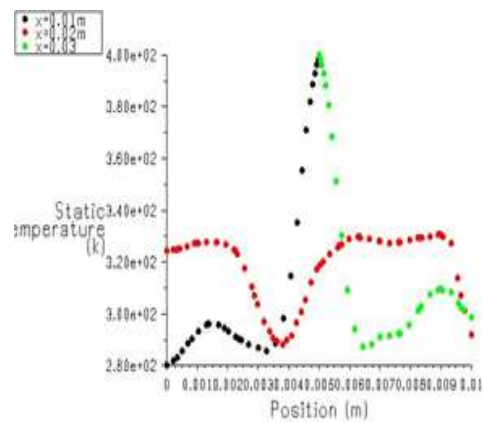
Static Temperature FLUENT 6.3 (2d, dp, pbns, iam) Sep 03,

Fig.6.5.4.D=0.8cm,m=0.20kg/s



Static Temperature FLUENT 6.3 (2d, dp, pbns, iam) Sep 03,

Fig.6.5.5.D=0.8cm,m=0.25kg/s



Static Temperature FLUENT 6.3 (2d, dp, pbns, iam) Sep 03,

Fig.6.5.6D=0.8cm,m=0.30kg/s

6.6 Static Pressure Variation in y-axis for different mass flow rates with diameter D=0.8cm

Here we are representing the resultant values for only one diameter i.e; D=0.8cm with different mass flow rate values (i.e; m=0.05, 0.10, 0.15, 0.20, 0.25, & 0.30kg/s) we got the other results for other diameters also but not representing here.

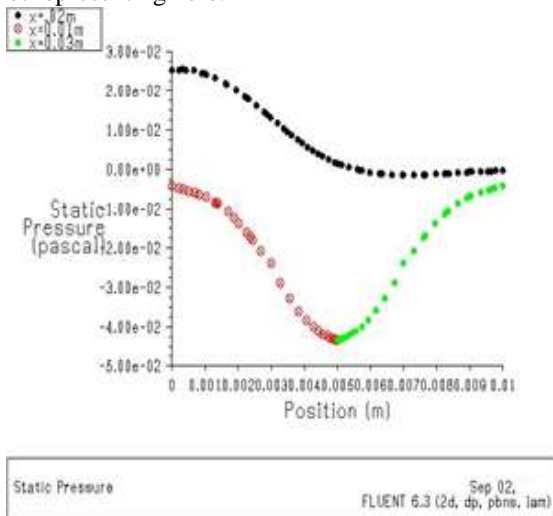


Fig.6.6.1.D=0.8cm,m=0.05kg/s

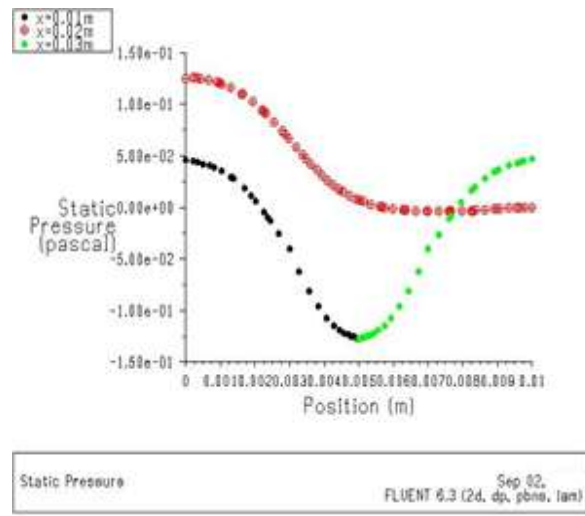


Fig.6.6.2.D=0.8cm,m=0.10kg/s

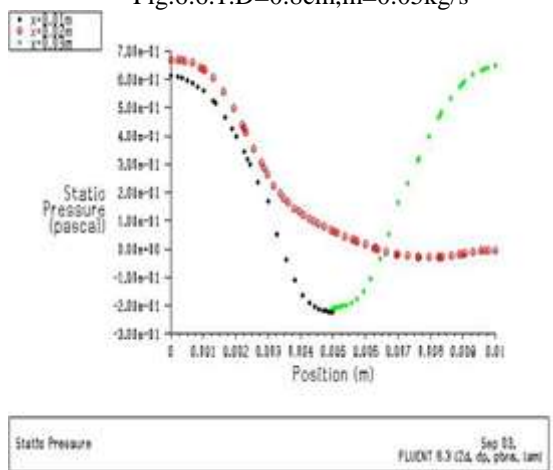


Fig.6.6.3.D=0.8cm,m=0.15kg/s

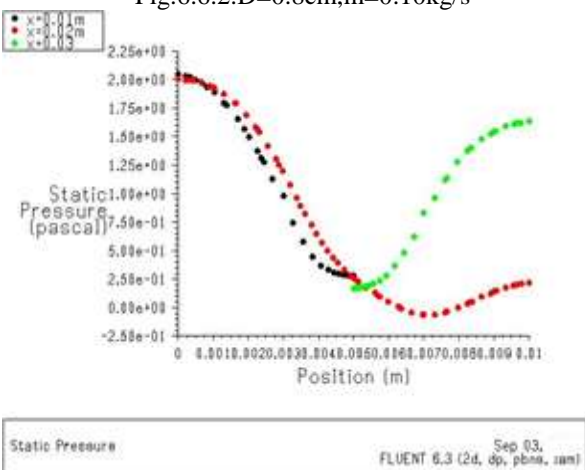


Fig.6.6.4.D=0.8cm,m=0.20kg/s

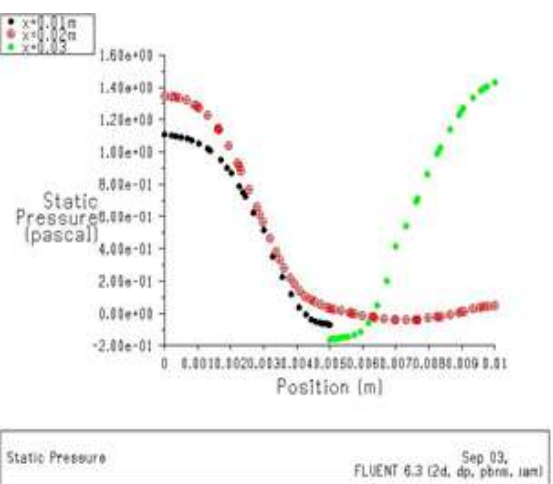


Fig.6.6.5.D=0.8cm,m=0.25kg/s

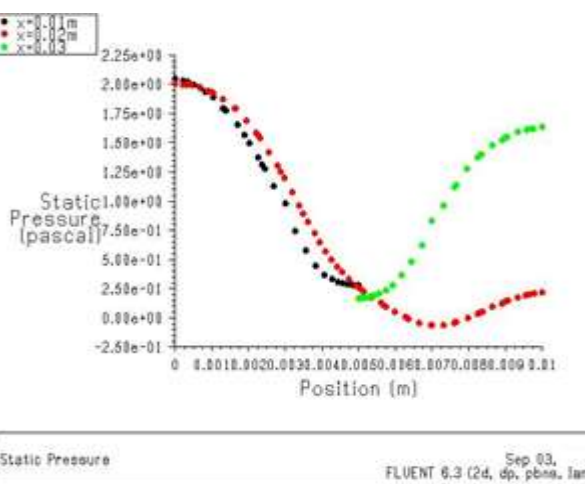


Fig.6.6.6.D=0.8cm,m=0.30kg/s

6.7 Nusselt number plot with different mass flow rates with diameter D=0.8cm

Here we are representing the resultant values for only one diameter i.e; $D=0.8\text{cm}$ with different mass flow rate values (i.e; $m=0.05, 0.10, 0.15, 0.20, 0.25, \& 0.30\text{kg/s}$) we got the other results for other diameters also but not representing here.

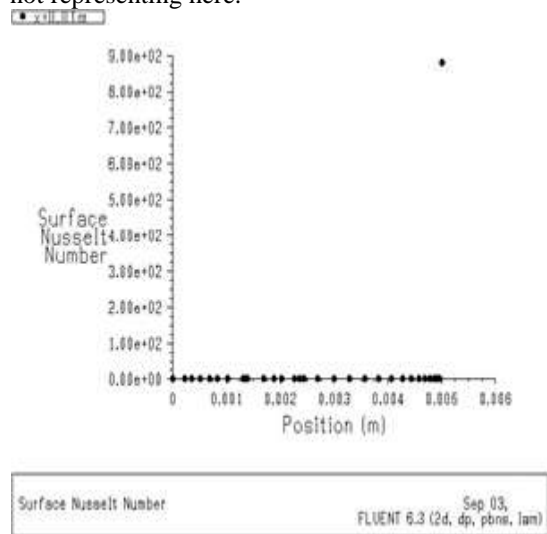


Fig.6.7.1.D=0.8cm,m=0.05kg/s

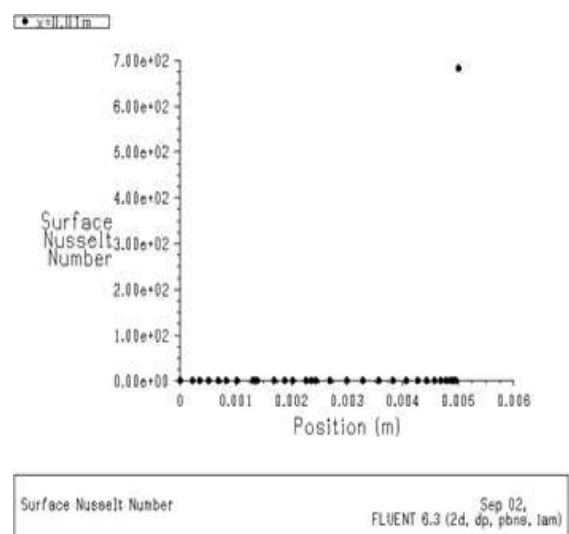


Fig.6.7.2D=0.8cm,m=0.10kg/s

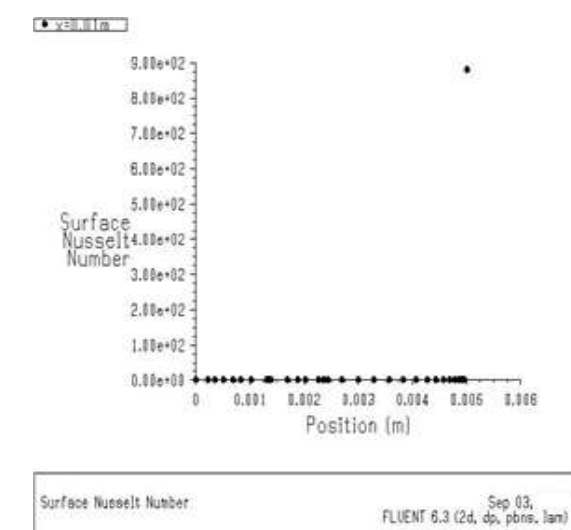


Fig.6.7.3.D=0.8cm,m=0.15kg/s

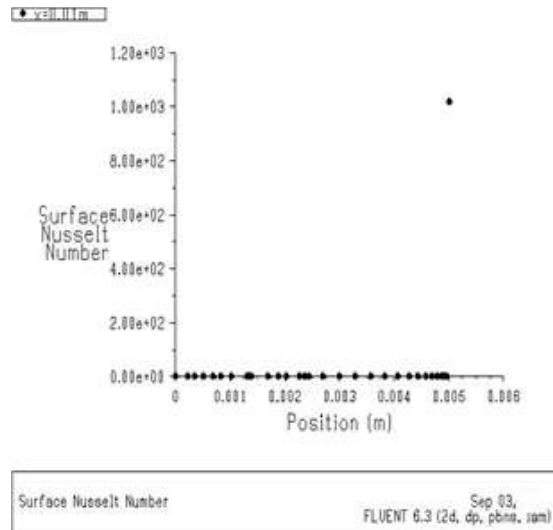


Fig.6.7.4.D=0.8cm,m=0.20kg/s

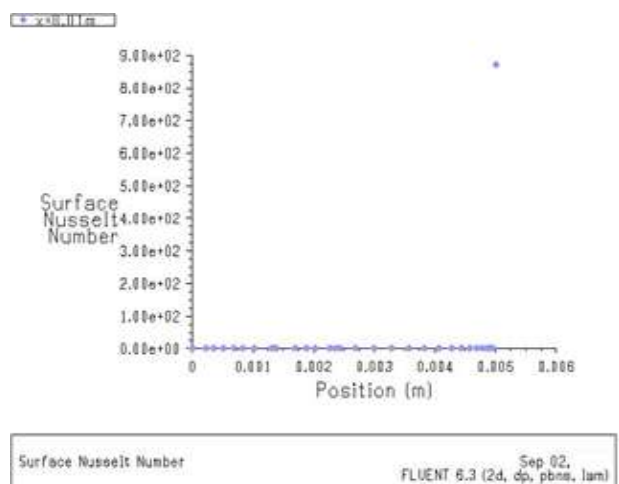
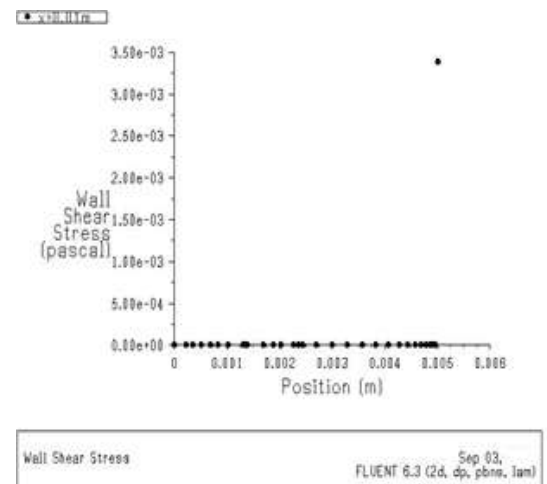


Fig.6.7.5.D=0.8cm,m=0.25kg/s

Fig.6.7.6.D=0.8cm,m=0.30kg/s

6.8 Verification of Results

6.8.1 Predicted values of FLUENT Vs Correlation for aluminium

Diameter (cm)	Mass flow rate (kg/s)	Max velocity(m/s)	ReD	Pr	NuD(corr)	NuD _{x=0.01}	%error
0.8	0.05	0.0115	91.559	6.99091	9.296	8.278	0.1095
	0.10	0.0238	189.488	6.99091	13.97	8.975	0.3575
	0.15	0.0382	304.137	6.99091	18.20	8.125	0.55405
	0.20	0.0512	407.639	6.99091	21.45	5.675	0.7356
	0.25	0.0654	520.690	6.99091	24.606	2.650	0.8923
	0.30	0.0795	632.95	6.99091	27.449	4.740	0.827
1.00	0.05	0.0095	94.544	6.99091	34.30	13.366	0.6114
	0.10	0.0201	200.03	6.99091	14.40	18.465	0.2198
	0.15	0.0324	322.44	6.99091	18.81	23.785	0.2208
	0.20	0.0425	422.96	6.99091	21.90	27.082	0.191
	0.25	0.0593	590.16	6.99091	24.89	27.750	0.1027
	0.30	0.0689	685.70	6.99091	28.707	28.590	0.00409
1.2	0.05	0.00752	89.808	6.99091	9.19	16.150	0.4305
	0.10	0.1625	194.066	6.99091	14.158	22.230	0.36309
	0.15	0.02534	302.62	6.99091	18.15	24.820	0.2684
	0.20	0.03675	438.889	6.99091	22.36	27.120	0.1755
	0.25	0.04635	553.53	6.99091	25.463	27.345	0.0688
	0.30	0.05780	690.28	6.99091	28.814	27.565	0.0433

6.8.2 Predicted values of FLUENT Vs Correlation for copper

Diameter (cm)	Mass flow rate (kg/s)	Max Velocity (m/s)	ReD	Pr	NuD(corr)	NuD _{x=0.01}	%error
0.8	0.05	0.011462	91.257	6.99091	9.279	8.72	0.0602
	0.10	0.0231	183.915	6.99091	13.738	8.95	0.3485
	0.15	0.0335	266.717	6.99091	16.99	7.84	0.536
	0.20	0.0502	399.67	6.99091	21.21	5.15	0.757
	0.25	0.0675	537.41	6.99091	23.62	2.45	0.896
	0.30	0.0819	652.06	6.99091	27.91	4.75	0.829
1.0	0.05	0.0092	91.55	6.99091	9.29	13.15	0.293
	0.10	0.019	189.09	6.99091	13.95	19.72	0.292
	0.15	0.0316	314.487	6.99091	18.55	23.82	0.2211
	0.20	0.0420	417.99	6.99091	21.75	25.94	0.1612
	0.25	0.0542	539.406	6.99091	25.09	27.45	0.0856
	0.30	0.0653	679.73	6.99091	28.94	27.12	0.062
1.2	0.05	0.00778	92.913	6.99091	9.37	16.00	0.4141
	0.10	0.0160	191.67	6.99091	14.06	23.82	0.4097
	0.15	0.0258	308.118	6.99091	18.34	24.88	0.2627
	0.20	0.0367	431.126	6.99091	22.13	25.87	0.144
	0.25	0.0466	556.52	6.99091	24.09	26.82	0.101
	0.30	0.0578	690.28	6.99091	28.81	27.02	0.0622

6.8.3 Predicted values of FLUENT Vs Correlation for (Ni-Cr alloy)

Diameter (cm)	Mass flow rate (kg/s)	Max velocity (m/s)	ReD	Pr	NuD(corr)	NuD _{x=0.01}	% Error
0.8	0.05	0.0103	82.005	6.99091	8.740	8.12	0.0709
	0.10	0.0227	180.730	6.99091	13.60	8.48	0.3760
	0.15	0.0363	289.010	6.99091	17.69	7.61	0.5701
	0.20	0.0512	417.990	6.99091	21.75	5.02	0.769
	0.25	0.0682	542.988	6.99091	25.19	2.532	0.8995
	0.30	0.0826	657.637	6.99091	28.04	4.940	0.823
1.0	0.05	0.00913	90.863	6.99091	9.256	13.00	0.6114

	0.10	0.0199	198.04	6.99091	14.32	18.245	0.2151
	0.15	0.0327	325.43	6.99091	17.45	23.567	0.2592
	0.20	0.0432	429.93	6.99091	22.10	27.254	0.1889
	0.25	0.0515	512.53	6.99091	24.36	27.89	0.1256
	0.30	0.0599	596.133	6.99091	26.543	28.674	0.0743
1.2	0.05	0.00783	93.510	6.99091	9.406	14.150	0.335
	1.00	0.01656	197.768	6.99091	14.309	19.532	0.267
	0.15	0.02534	302.62	6.99091	18.15	24.820	0.2684
	0.20	0.0383	457.400	6.99091	22.88	27.12	0.156
	0.25	0.0498	594.74	6.99091	26.508	28.645	0.0746
	0.30	0.05245	626.86	6.99091	27.289	29.565	0.67769

For better understanding of theoretical values and simulation values for different diameters and mass flow rates, the following graphs are drawn.

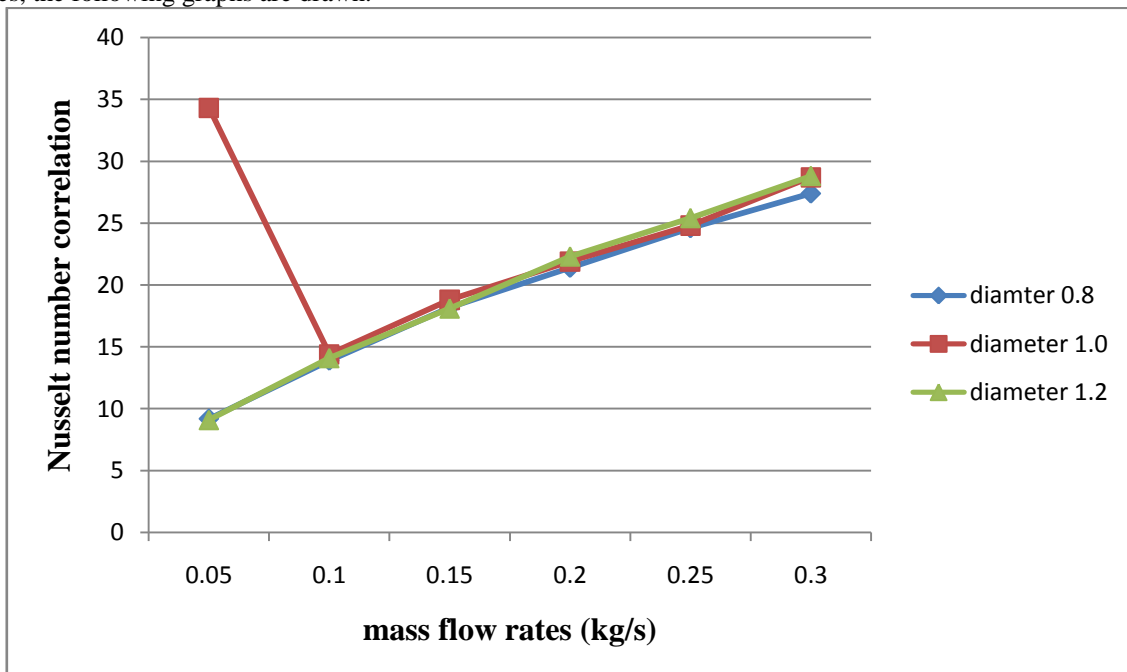


Figure 6.8.1 mass flow rates V_s Nusselt number for Aluminium tubes

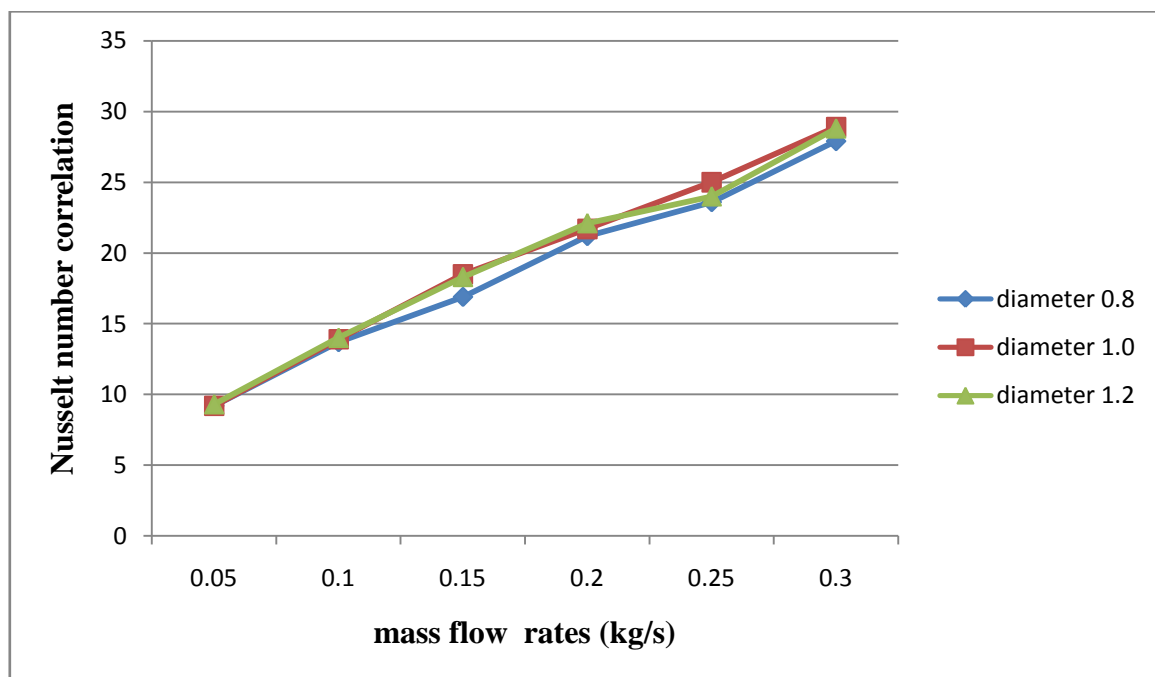


Figure 6.8.2 mass flow rate V_s Nusselt number for copper tubes.

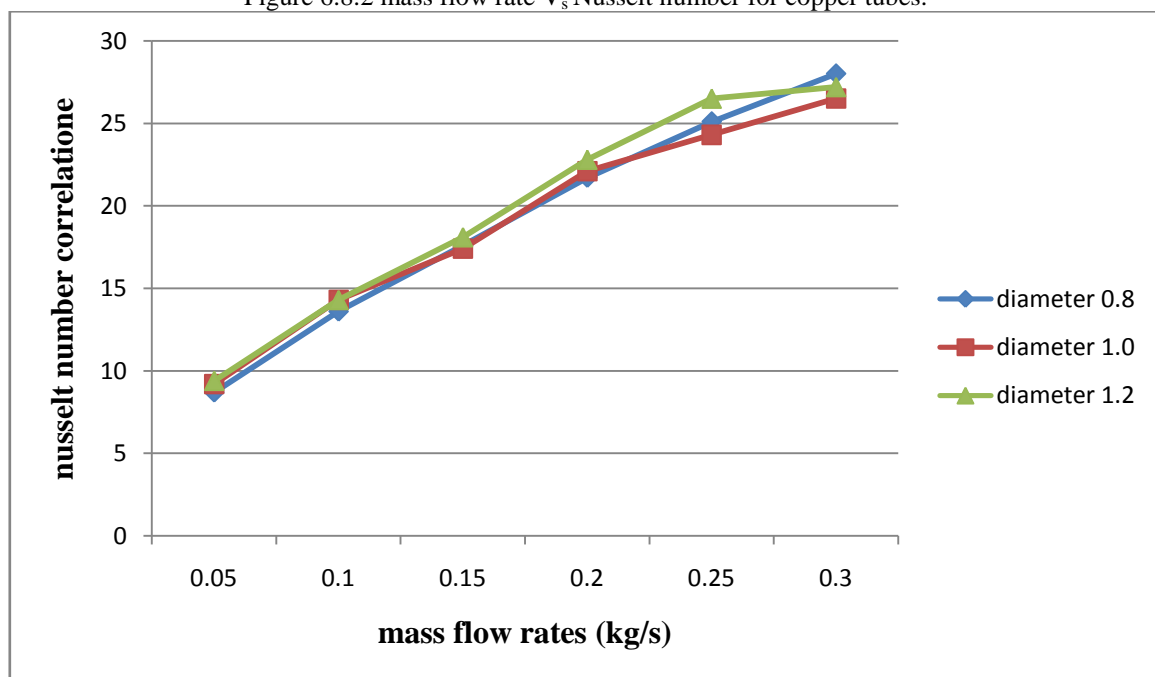


Figure 6.8.3 mass flow rate V_s Nusselt number correlation for Nickel-Chromium base super alloy base tube.

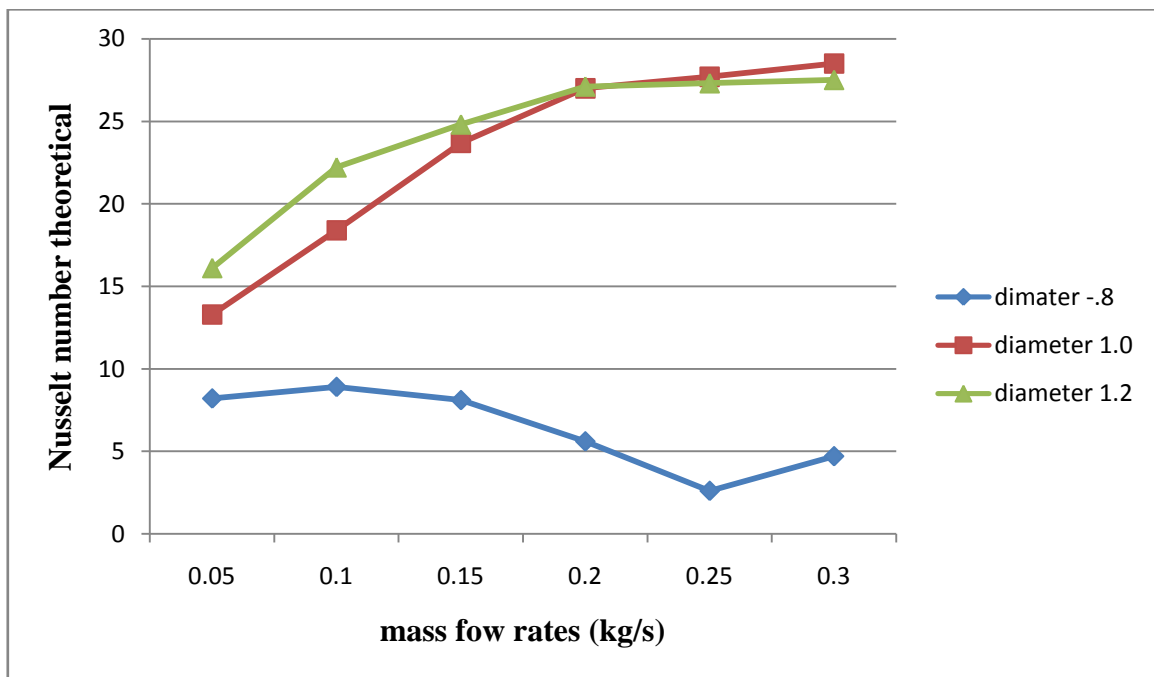


Figure 6.8.4 mass flow rate V_s Nusselt number theoretical for aluminium

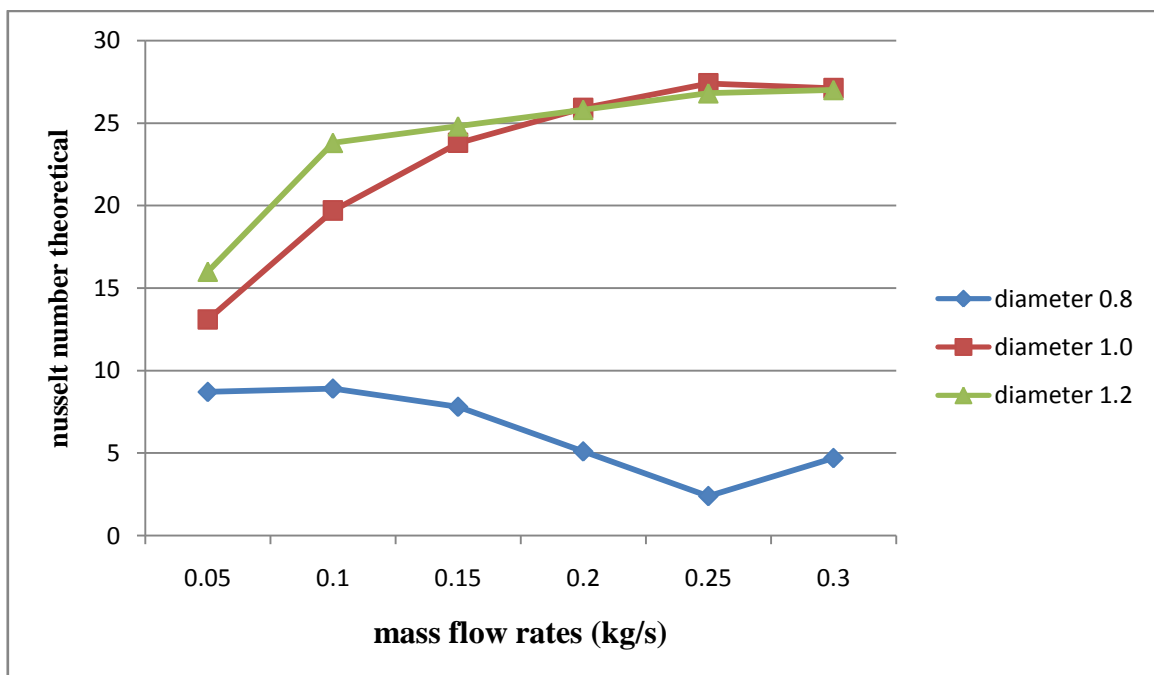


Figure 6.8.5 mass flow rates V_s Nusselt number theoretical for copper tubes.

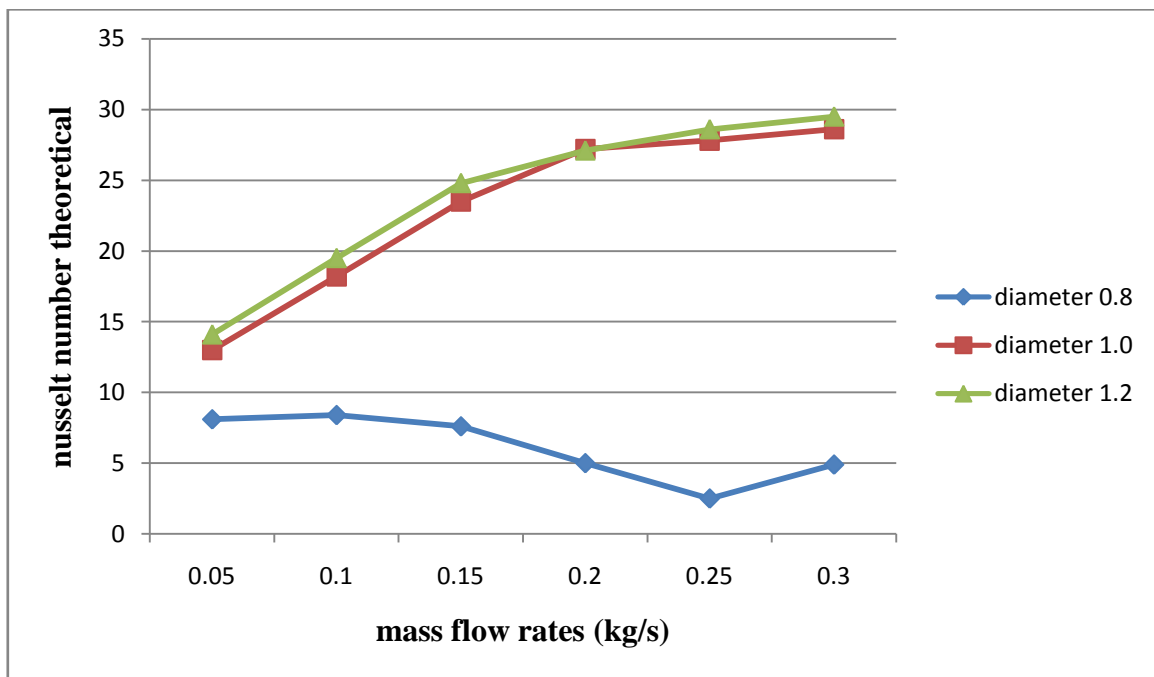


Figure 6.8.6 mass flow rates V_s Nusselt number theoretical for Nickel- chromium base super alloy.

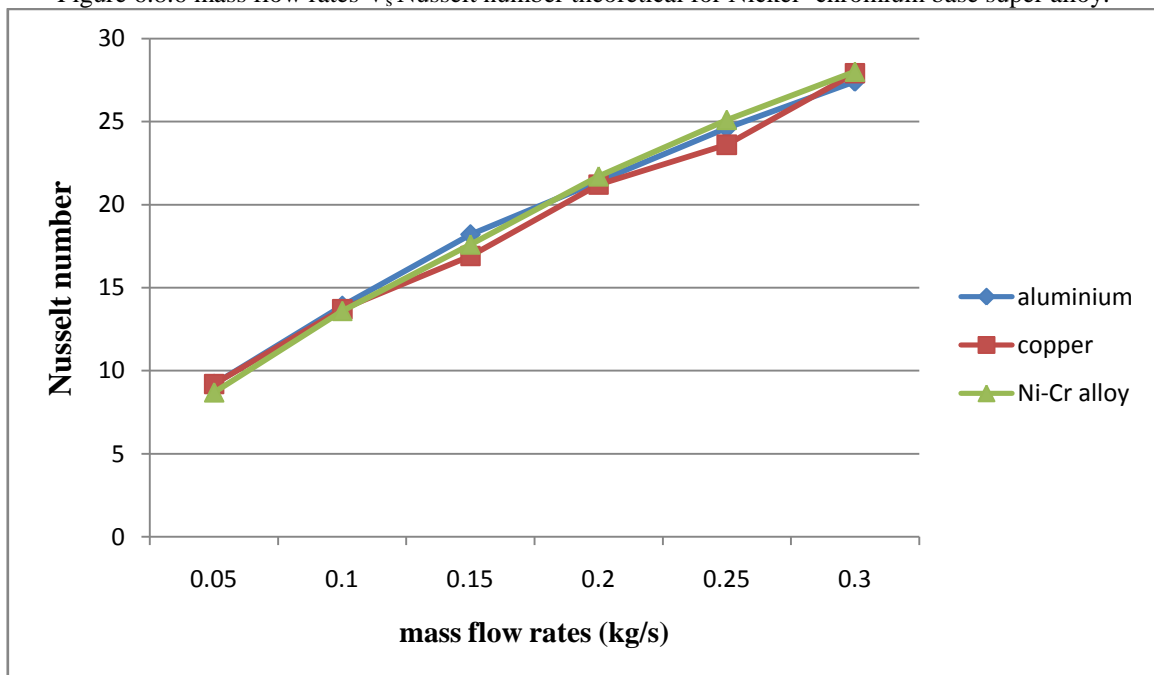


Figure 6.8.7 mass flow V_s Nusselt number for different materials at $d=0.08\text{cm}$

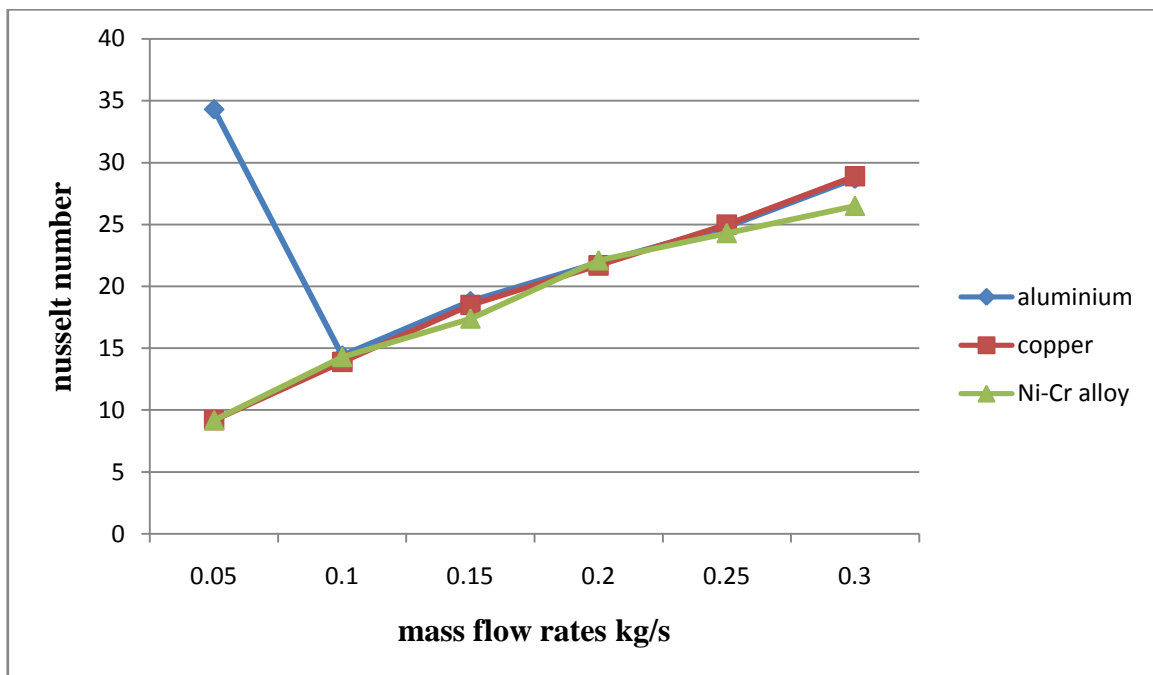


Figure 6.8.8 mass flow rates Vs Nusselt number for different materials at d=1.0cm

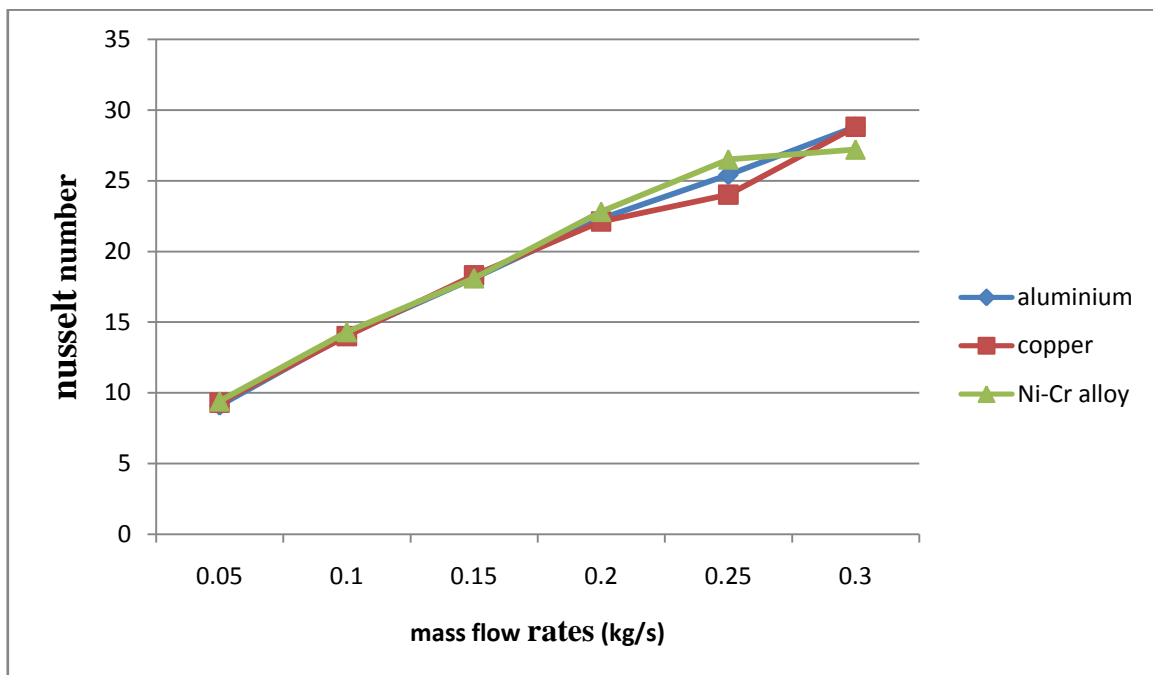


Figure 6.8.9 mass flow rates Vs mass flow rates for different materials at d=1.20cm

- From the above graphs the observations are:
- The effect of different mass flow rates on both flow and heat transfer is significant. It was observed that 1.0cm diameter of tubes and 0.05kg/s mass flow gives the best results as 34.30 Nusselt number.
 - From the above graphs we can observe that alloys serves as a better material for tube when compare with copper and aluminium.
 - The effect of mass flow rates on both flow and heat transfer is significant. This is due to variation of space of the surrounding tubes.
 - It was observed optimal flow distribution was found for 0.8cm diameter and 0.05kg/s mass flow rate in case of alloy.

VII. Conclusions

Mode and mesh creation in CFD is one of the most important phases of simulation. The model and mesh density determine the accuracy and flexibility of the simulations. Too dense a mesh will unnecessarily increase the solution time; too coarse a mesh will reach to a divergent solution quickly. But will not show an accurate flow profile. An optimal mesh is denser in areas where there are no flow profile changes.

- A two-dimensional numerical solution of flow and heat transfer in a bank of tubes which is used in industrial applications has been carried out.
- Laminar flow past a tube bank is numerically simulated in the low Reynolds number regime. Velocity vector depicts zones of recirculation between the tubes. Nusselt number variations are obtained and pressure distribution along the bundle cross section is presented.
- The effect of different mass flow rates on both flow and heat transfer is significant. This is due to the variation of space of the succeeding rows of tubes. It was observed that 1.0cm diameter of tubes and 0.05kg/s mass flow rate gives the best results.
- Mass flow rate has an important effect to heat transfer. An optimal flow distribution can result in a higher temperature distribution and low pressure drop. It was observed that the optimal flow distribution was occurred in 1.0cm diameter and 0.05kg/s mass flow rate.
- CFD simulations are a useful tool for understanding flow and heat transfer principles as well as for modelling these types of geometries.
- It was observed that 1.0cm diameter of tubes and 0.30kg/s mass flow rate yields optimum results for aluminium as tube material, where as it was observed that 0.8cm and 0.05kg/s mass flow rate in case of copper tube material.
- From the above graphs we observed that alloys serves as a better material for tube compared with copper and aluminium.
- Alloy (Nickel-Chromium based) serves as a better material for heat transfer applications with low cost
- Further improvements of heat transfer and fluid flow modelling can be possible by modelling three dimensional models and changing the working fluid.
- It was observed that Heat transfer rate is more for Nano fluids when compared to water.

References

- [1.] Patankar, S.V. and Spalding, D.B. (1974), "A calculation for the transient and steady state behaviour of shell- and- tube Heat Exchanger". Heat transfer design and theory sourcebook. Afgan A.A. and Schluner E.U.. Washington. Pp. 155-176.
- [2.] Kelkar, K.M and Patankar, S. V., 1987 "Numerical prediction of flow and Heat transfer in a parallel plate channel with staggered fins", Journal of Heat Transfer, vol. 109, pp 25-30.
- [3.] Berner, C., Durst, F. And McEligot, D.M., "Flow around Baffles", Journal of Heat Transfer, vol. 106 pp 743-749.
- [4.] Popiel, C.O & Vander Merwe, D.F., "Friction factor in sine-pipe flow, Journal of fluids Engineering", 118, 1996, 341-345.
- [5.] Popiel, C.O & Wojkowiak, J., "friction factor in U-type undulated pipe flow, Journal of fluids Engineering", 122, 2000, 260-263.
- [6.] Dean, W. R., Note on the motion of fluid in a curved pipe, The London, Edinburgh and Dublin philosophical Magazine, 7 (14), 1927, 208-223.
- [7.] Patankar, S.V., Liu, C.H & Sparrow, E.M., "Fully developed flow and Heat Transfer in ducts having streamwise periodic variation in cross-sectional area", Journal of Heat Transfer, 99, 1977, 180-186.
- [8.] Webb, B.W & Ramdhyani, S., "Conjugate Heat Transfer in an channel with staggered Ribs" Int. Journal of Heat and Mass Transfer 28(9), 1985, 1679-1687.
- [9.] Park, K., Choi, D-H & Lee, K-s., "design optimization of plate heat exchanger with staggered pins", 14th Int. Symp.on Transport phenomena, Bali, Indonesia, 6-9 July 2003.
- [10.] N.R. Rosaguti, D.F. Fletcher & B.S. Haynes "Laminar flow in a periodic serpentine". 15th Australasian fluid mechanics conference. The University of Sydney, Sydney, Australia 13-17 December 2004.
- [11.] L.C Demartini, H.A. Vielmo, S.V. Moller "Numeric and experimental analysis of turbulent flow through a channel with baffle plates", J. Braz. Soc. Mech.Sci& Eng. Vol 26 No.2 Rio de Janeiro Apr/June 2004.
- [12.] Baier, G., Grateful, T.M. Graham, M.D. & Lightfoot E.N.(1999), " Prediction of mass transfer rates in spatially periodic flow", Chem. Eng. Sci., 54, 343-355.
- [13.] Bao, L. & Lipscomb, G.G., 2002 " Well-developed mass transfer in axial flows through randomly packed fiber bundles with constant wall flux", Chem. Eng. Sci., 57, 125-132.
- [14.] Launder, B.E. & Massey, T.H 1978 "The numerical predictions of viscous flow and heat transfer in tube bank". J. Heat transfer, 100, 565-571.
- [15.] Wung, T.S. & Chen, C.J. (1989), "Finite analytic solution of convective Heat transfer

- for tube arrays in cross flow: part- I flow field analysis”, ASME J. Heat Transfer, 111, 633-640.
- [16.] Schoner, P., Plucinski, W.N. & Daiminger, U. (1998), “Mass transfer in the shell side of cross flow hollow fiber modules”, Chem. Eng. Sci. 53, 2319-2326.
- [17.] T.Li, N.G. Deen & J.A D.G. M. Kuipers, faculty of Sci. & Tech, University of Twente, “Numerical study of Hydrodynamics and mass transfer of in line fiber arrays in laminar cross flow”, 3rd International conference on CFD in the Minerals and process Industries CSIRO, Melbourne, Australia 10-12 December 2003, pg, 87-92.
- [18.] T.V. Mull, Jr., M.W. Hopkins and D.G. White “Numerical Simulation Models for a Modern Boiler Design “, Power-Gen International’ 96, December 4-6, 1996, Orlando, Florida, U.S.A
- [19.] ["Enhancing the efficiency of polymerase chain reaction using graphene Nano flakes - Abstract- Nanotechnology - IOPscience" iop.org. Retrieved 8 June 2015.](#)
- [20.] ["Light: Science & Applications - Abstract of article: Nano fluid-based optical filter optimization for PV/T systems". nature.com. Retrieved 8 June 2015.](#)
- [21.] Shima P.D. and J. Philip (2011). "Tuning of Thermal Conductivity and Rheology of Nano fluids using an External Stimulus". J. Phys. Chem. C 115: 20097–20104. doi:10.1021/jp204827q.
- [22.] ["A review on preparation methods and challenges of Nano fluids". Sciencedirect.com. Retrieved 8 June 2015.](#)
- [23.] Chung, Y.M., Tucker, P.G., “Assessment of periodic flow assessment for unsteady state Heat Transfer in grooved channels; Transaction of the ASME, Vol.126, Dec (2004).